ELSEVIER

Agricultural and Forest Meteorology 100 (2000) 103–125

AGRICULTURAL AND FOREST METEOROLOGY

www.elsevier.com/locate/agrformet

Sources of errors in measurements of PAR

J. Ross *, M. Sulev

Tartu Observatory, Toravere, 61602 Tartumaa, Estonia

Received 4 May 1999; received in revised form 1 October 1999; accepted 9 October 1999

Abstract

Due to optical processes in the atmosphere the spectral distribution of global, direct solar and diffuse radiation is different and depends on solar elevation, atmosphere transparency etc. Because of various optical properties of phytoelements, the spectral distribution of penetrated and reflected radiation differs from that of incoming radiation. Owing to radiative transfer processes, photosynthetically active radiation (PAR) and its proportion in integral solar radiation is not constant. The aim of the paper is to study theoretically these changes and to estimate systematic errors caused by deviation of the spectral sensitivity of pyranometers and PAR sensors from the spectral sensitivity of ideal sensors.

The spectral distribution of radiation was estimated by combining different literature data and the spectral sensitivity of a typical pyranometer using available data for spectral transparency of glass domes and spectral reflectivity of black paints.

Simultaneous use of energetic and quantum treatments of radiation in biogeophysics and subsequent existence of different definitions of PAR is a source of uncertainties and misunderstanding. The basic concepts, units and conversion factors between integral radiation and PAR, as well PAR efficiency for different kinds of solar radiation, and spectral corrections for some radiation sensors will be discussed below.

Our calculations show that the conversion factor U_{PAR} is 1–3% higher for penetrated radiation and about 6% higher for reflected radiation compared with $U^{\mathrm{Q}}_{\mathrm{PAR}} = 0.219\,\mathrm{W\,s\,\mu mol^{-1}}$ for global radiation under a cloudless sky.

Due to the different spectral sensitivity of ideal energetic and ideal quantum sensors for PAR, the radiation measured through them differs 3–13% depending on the kind of radiation. Hence PAR quantum efficiency is 3–13% higher when PAR is defined as measured by the ideal energetic PAR sensor than when it is estimated by the ideal quantum PAR sensor. Their quantum efficiency depends essentially on the kind of radiation: for diffuse radiation it is increased by 13% but for reflected radiation it is decreased to about one fourth compared with global and direct solar radiation. For penetrated global radiation, quantum efficiency decreases rapidly with canopy depth, being 8–9 times lower at the bottom of a dense canopy than above it.

For the LI-COR LI-190SA Quantum Sensor, systematic spectral errors do not exceed 1%. For the Kipp and Zonen PAR LITE sensor, errors are between 1 and 8% depending on the kind of radiation. For the LI-COR LI-200SA Pyranometer Sensor, systematic spectral errors for the global radiation reflected or penetrated by the canopy are high (20–40%), and this instrument cannot be recommended for measurements inside the canopy as is warned also by the manufacturers.

Keywords: PAR quantum sensor; Pyranometer; PAR measurement; Spectral errors; Relation between PAR and integral radiation

1. Introduction

Before discussing how to measure photosynthetically active radiation (PAR) it should be clarified and

* Corresponding author. Tel.: +372-7-410-278; fax: +372-7-410-205.
E-mail address: ross@aai.ee (J. Ross).

0168-1923/00/$ – see front matter
PII: S0168-1923(99)00144-6

agreed upon as to what PAR is. In general use, PAR is defined as radiation within the range of wave lengths 400 and 700 nm, or 380 and 710 nm (e.g. Gaastra, 1959; Nichiporovich, 1960; McCree, 1966). Such a definition is vague and indefinite as was first pointed out by McCree (1972a). The wave length band of 400–700 nm, commonly accepted at present, does not cause misunderstanding. Another, more serious, problem is how PAR is defined inside this wave length band. The expression "... radiation between 400 and 700 nm..." would lead physicists and actinometrists to the idea that radiation (radiation flux density) inside this band must be measured nonselectively (irrespective of wave length) by the ideal PAR energetic sensor. Biologists and plant physiologists treat PAR as photon flux density which must be measured nonselectively in the PAR spectral region. According to this interpretation, PAR is to be measured using the ideal PAR quantum sensor, i.e. the sensor whose spectral sensitivity between 400 and 700 nm is proportional to wave length. These two conceptions are in principle different and this should be taken into account in theoretical treatments and especially in analysing or comparing experimental data (McCree, 1973). Since the authors avoid preferring one definition to the other, the problems of PAR measurement will be considered, after a brief historical overview, in parallel following two possible definitions.

There exists no worldwide network for PAR measurements like the network of actinometric stations, where global, direct, diffuse and reflected solar radiation are measured using unified instruments and methodology and are metrologically based on the World Radiometric Reference (Romero et al., 1996). The problem becomes more complicated when it is necessary to measure PAR. In the Western countries, PAR is defined as radiation in the spectral interval 400–700 nm (e.g. Gaastra, 1959; McCree, 1972a, b). In the former Soviet Union and socialist countries, PAR was defined as radiation between 380 and 710 nm (Nichiporovich, 1960; Tooming and Gulyayev, 1967; Ross, 1981). Due to this difference, PAR data originating from the former socialist countries (e.g. Moldau et al., 1963; Yefimova, 1965) are augmented 5–7% (Tooming and Gulyayev, 1967).

It is possible to estimate PAR theoretically by integrating the spectral irradiance $I(\lambda)$ determined from model calculations over the PAR wave length interval 400–700 nm. It was first done by McCree (1972a) who used for $I(\lambda)$ the data of Henderson and Hodgkiss (1963). Later the models of global and diffuse radiation of Avaste et al. (1962) were used by Moldau et al. (1963) and McCree (1976). The SPECTRAL2 model of Bird and Riordan (1986) was used by Olseth and Skartveit (1997).

PAR measurements, carried out with different sensors and measuring systems, can be divided into three groups:

1. Measurements of spectral irradiance of global, direct, diffuse and reflected solar radiation using spectroradiometers (e.g. Niilisk, 1962, 1965; Scott et al., 1968; Bird et al., 1982; Ross et al., 1986; Lee and Graham, 1986; Deering and Leone, 1986; Pearcy, 1989; Gueymard, 1989; Endler, 1993; Czarnowski, 1994a, b) and estimation of PAR by integrating spectral irradiance over the region 400–700 nm.
2. Measurements of global, diffuse or reflected PAR by pyranometers covered with hemispherical glass filters WG295 and RG695 (e.g. McCree, 1966; Rodskjer and Kornher, 1971; Stanhill and Fuchs, 1977; Stigter and Musabilha, 1982; Blackburn and Proctor, 1983; Hansen, 1984; Rao, 1984; Spitters et al., 1986; Slomka and Slomka, 1986), or measurements of direct solar PAR by pyrheliometers covered with identical flat filters (Tooming and Niilisk, 1967; Karalis, 1989; Jacovides et al., 1993).
3. Measurements of global, diffuse or reflected PAR with sensors based on silicon photodiodes. Following mass production of quantum sensors LI-190SA (silicon photodiode covered with a visible bandpass interference filter and a coloured glass filter) by LI-COR (LI-COR, 1986; 1991) use of quantum sensors has been rapidly expanded (e.g. Norman et al., 1969; Britton and Dodd, 1976; Howell et al., 1983; Pearcy, 1989; Alados et al., 1995; Ross et al., 1998).

Due to different sensors and measurement methods the obtained data are not fully comparable and include various systematic errors. Therefore the problem of the calculation of PAR using the data of integral solar radiation has retained its use, and conversion from integral radiation to PAR is widely discussed (e.g. Moldau et al., 1963; Tooming and Gulyayev, 1967; Britton and Dodd, 1976; Ross, 1981; Rao, 1984; Meek et al., 1984;

Alados et al., 1995; Sulev and Ross, 1996). The values of PAR can be expressed in energy units ($W\,m^{-2}$) or in photobiological units ($\mu mol\,m^{-2}\,s^{-1}$); however, conversion from one set of units to the other needs special care because it depends on the spectral composition of the measured radiation (Sulev and Ross, 1996).

Spectral sensitivity of real PAR sensors corresponds only approximately to that of the ideal PAR sensor (Li-COR, Instruction Manual, 1986; Pearcy, 1989), and in data processing the use of different correction factors appears necessary. These factors depend on the spectral sensitivity of the sensor as well on the spectral distribution of the measured radiation. Therefore, to obtain the most accurate values of PAR, various methodological problems have to be solved when one determines the different conversion factors and correction coefficients. In this paper the methodological basis for determination of PAR is elaborated, formulae for calculation of different conversion factors and correction coefficients are derived and the results from the calculations are discussed.

2. Basic concepts

Radiant energy is one of the many interchangeable forms of energy which plays an important role in different natural processes in the atmosphere, ground surface and plant canopy. A great deal of confusion has existed regarding the treatment and measurement of radiation, especially when emphasis is placed not on the energetic but some other aspect of radiation.

2.1. Terminology and units

The basic quantity in radiometry is spectral irradiance (radiant flux density) $I(\lambda)$, which is radiant flux taken over an infinitesimal spectral range on either side of wavelength λ incident per unit area of surface. The SI (International System of Units) unit of radiant flux is the watt (W) and, consequently, the unit of spectral irradiance is $W\,m^{-2}\,nm^{-1}$. In the plant sciences, quantum units are commonly used for radiation. However, there is no official SI unit of photon flux. The mole of photons and the einstein are usually employed to designate Avogadro's number of photons. While the einstein was applied in the plant sciences initially, the use of the mole is to be recommended since it is an SI unit. Accordingly, $\mu mol\,m^{-2}\,s^{-1}\,nm^{-1}$ is a convenient quantum unit for spectral irradiance (spectral photon flux density). To avoid misunderstanding, radiant quantities in energy units are marked below with the superscript index E and those in quantum units with the index Q.

These two unit systems are not independent but are linked through Planck's law $E = hc/\lambda$; the relation between spectral irradiance in quantum units $I^{Q}(\lambda)$ and the same irradiance in energy units $I^{E}(\lambda)$ can be expressed as

$$I^{Q}(\lambda) = \frac{\lambda I^{E}(\lambda)}{N_A hc} = \frac{\lambda I^{E}(\lambda)}{\gamma}, \tag{1}$$

where h is Planck's constant ($h = 6.63 \times 10^{-34}\,W\,s$), c is velocity of light ($c = 3 \times 10^{8}\,m\,s^{-1}$), λ is wave length in nm, N_A is Avogadro's quantity ($1\,\mu mol\,s^{-1}\,m^{-2} = 6.022 \times 10^{17}$ photons $s^{-1}\,m^{-2}$) and $\gamma = N_A hc$ ($\gamma = 119.8\,W\,s\,nm\,\mu mol^{-1}$).

More often, it is not spectral irradiance $I(\lambda)$ but integral irradiance over the spectral interval from λ_{min} to λ_{max}

$$I = \int_{\lambda_{min}}^{\lambda_{max}} I(\lambda)\,d\lambda \tag{2}$$

that is required. There are two possible treatments depending on how integral (Eq. (2)) is interpreted.

2.2. Energy treatment

Energy based treatment is used when the energy aspect of radiation is required (e.g. energy transfer and transformation in the atmosphere and at the ground surface etc.) and it is based on the wave nature of radiation. Integral irradiance is defined as

$$I_E^{E} = \int_{\lambda_{min}}^{\lambda_{max}} I^{E}(\lambda)\,d\lambda \tag{2a}$$

and, to be exact, it should be called integral energy irradiance in energy units. It is possible to express integral energy irradiance also in quantum units using Eq. (1) (although it is rarely used)

$$I_E^{Q} = \frac{1}{\gamma}\int_{\lambda_{min}}^{\lambda_{max}} \lambda I^{E}(\lambda)\,d\lambda. \tag{2b}$$

One can see that spectral irradiance in energy units $I^{\mathrm{E}}(\lambda)$ is integrated here with the weight proportional to wave length λ.

According to the definition of energy irradiance given by Eq. (2a) one can define the ideal energy sensor for measuring $I_{\mathrm{E}}^{\mathrm{E}}$ as a sensor which measures spectral irradiance $I^{\mathrm{E}}(\lambda)$ equally (not depending on wave length λ) over spectral region from $\lambda_{\min}$ to $\lambda_{\max}$ where the radiation $I^{\mathrm{E}}(\lambda)$ differs from zero.

When measuring $I^{\mathrm{E}}(\lambda)$ we assumed that the sensor's electrical output $n_{\mathrm{E}}(\lambda)$ is proportional to $I^{\mathrm{E}}(\lambda)$

$$n_{\mathrm{E}}(\lambda) = \varepsilon_{\mathrm{E}}^{\mathrm{E}}(\lambda) I^{\mathrm{E}}(\lambda), \tag{3}$$

where the proportionality factor $\varepsilon_{\mathrm{E}}^{\mathrm{E}}(\lambda)$ is the spectral sensitivity of energy sensors in energy units. It characterizes the optical and electrical parameters of the sensor and depends generally on wave length λ. Only for the ideal energy sensor, spectral sensitivity will be constant and we can write

$$\varepsilon_{\mathrm{idE}}^{\mathrm{E}}(\lambda) = \mu_{\mathrm{E}} = \text{const}. \tag{4}$$

When measuring the integral irradiance $I_{\mathrm{E}}^{\mathrm{E}}$ in energy units over the whole spectral interval from $\lambda_{\min}$ to $\lambda_{\max}$ the integral electrical output n_{E} of the energy sensor is

$$n_{\mathrm{E}} = \int_{\lambda_{\min}}^{\lambda_{\max}} n_{\mathrm{E}}(\lambda)\,\mathrm{d}\lambda = \int_{\lambda_{\min}}^{\lambda_{\max}} \varepsilon_{\mathrm{E}}^{\mathrm{E}}(\lambda) I^{\mathrm{E}}(\lambda)\,\mathrm{d}\lambda. \tag{5}$$

Integral sensitivity of the energy sensor in energy units is defined as

$$\varepsilon_{\mathrm{E}}^{\mathrm{E}} = \frac{n_{\mathrm{E}}}{I^{\mathrm{E}}} = \frac{\int_{\lambda_{\min}}^{\lambda_{\max}} \varepsilon_{\mathrm{E}}^{\mathrm{E}}(\lambda) I^{\mathrm{E}}(\lambda)\mathrm{d}\lambda}{\int_{\lambda_{\min}}^{\lambda_{\max}} I^{\mathrm{E}}(\lambda)\mathrm{d}\lambda}. \tag{6}$$

According to Eqs. (5) and (6) one has for the ideal energy sensor

$$n_{\mathrm{idE}} = \mu_{\mathrm{E}} I^{\mathrm{E}}; \qquad \varepsilon_{\mathrm{idE}}^{\mathrm{E}} = \mu_{\mathrm{E}}. \tag{7}$$

To collate the spectral sensitivity $\varepsilon_{\mathrm{E}}^{\mathrm{E}}(\lambda)$ of different energy sensors the relative spectral sensitivity

$$\bar{\varepsilon}_{\mathrm{E}}^{\mathrm{E}}(\lambda) = \frac{\varepsilon_{\mathrm{E}}^{\mathrm{E}}(\lambda)}{\varepsilon_{\mathrm{idE}}^{\mathrm{E}}(\lambda)} = \frac{\varepsilon_{\mathrm{E}}^{\mathrm{E}}(\lambda)}{\mu_{\mathrm{E}}} \tag{8}$$

is used. From Eqs. (4) and (6) it follows that $\bar{\varepsilon}_{\mathrm{idE}}^{\mathrm{E}}(\lambda) \equiv 1$.

Following Eqs. (6) and (8) the integral output of the energy sensor in measuring the irradiance $I^{\mathrm{E}}(\lambda)$, is

$$n_{\mathrm{E}} = \mu_{\mathrm{E}} \int_{\lambda_{\min}}^{\lambda_{\max}} \bar{\varepsilon}_{\mathrm{E}}^{\mathrm{E}}(\lambda) I^{\mathrm{E}}(\lambda)\mathrm{d}\lambda \tag{5a}$$

and integral sensitivity in energy units $\varepsilon_{\mathrm{E}}^{\mathrm{E}}$ is

$$\varepsilon_{\mathrm{E}}^{\mathrm{E}} = \frac{n_{\mathrm{E}}}{I^{\mathrm{E}}} = \frac{\mu_{\mathrm{E}} \int_{\lambda_{\min}}^{\lambda_{\max}} \bar{\varepsilon}_{\mathrm{E}}^{\mathrm{E}}(\lambda) I^{\mathrm{E}}(\lambda)\mathrm{d}\lambda}{I^{\mathrm{E}}}. \tag{6a}$$

The relation

$$\beta_{\mathrm{E}}^{\mathrm{I}} = \frac{n_{\mathrm{E}}}{n_{\mathrm{idE}}} = \frac{\int_{\lambda_{\min}}^{\lambda_{\max}} \bar{\varepsilon}_{\mathrm{E}}^{\mathrm{E}}(\lambda) I^{\mathrm{E}}(\lambda)\mathrm{d}\lambda}{I^{\mathrm{E}}} \tag{9}$$

can be considered the spectral correction of the integral sensitivity of the real energy sensor relative to the ideal one in measuring radiation I^{E}.

2.3. Quantum treatment

Quantum treatment of radiation, based on the quantum nature of radiation, is preferred when the quantum effect of radiation or the total number of photons is essential. The integral quantum irradiance $I_{\mathrm{Q}}^{\mathrm{Q}}$ in quantum units is

$$I_{\mathrm{Q}}^{\mathrm{Q}} = \int_{\lambda_{\min}}^{\lambda_{\max}} I^{\mathrm{Q}}(\lambda)\mathrm{d}\lambda. \tag{2c}$$

Analogously to the energy treatment proceeding from Eq. (2c), one can define the ideal quantum sensor as a sensor which measures spectral irradiance expressed in quantum units irrespective of the wave length λ.

The electrical output of the quantum sensor is

$$n_{\mathrm{Q}}(\lambda) = \varepsilon_{\mathrm{Q}}^{\mathrm{Q}}(\lambda) I^{\mathrm{Q}}(\lambda), \tag{3a}$$

where $\varepsilon_{\mathrm{Q}}^{\mathrm{Q}}(\lambda)$ is the spectral sensitivity of the quantum sensor in quantum units. When measuring the integral quantum irradiance I^{Q} the integral output of the quantum sensor n_{Q} is

$$n_{\mathrm{Q}} = \int_{\lambda_{\min}}^{\lambda_{\max}} n_{\mathrm{Q}}(\lambda)\mathrm{d}\lambda = \int_{\lambda_{\min}}^{\lambda_{\max}} \varepsilon_{\mathrm{Q}}^{\mathrm{Q}}(\lambda) I^{\mathrm{Q}}(\lambda)\mathrm{d}\lambda \tag{5b}$$

and its integral sensitivity in quantum units is

$$\varepsilon_{\mathrm{Q}}^{\mathrm{Q}} = \frac{n_{\mathrm{Q}}}{I^{\mathrm{Q}}} = \frac{\int_{\lambda_{\min}}^{\lambda_{\max}} \varepsilon_{\mathrm{Q}}^{\mathrm{Q}}(\lambda) I^{\mathrm{Q}}(\lambda)\mathrm{d}\lambda}{\int_{\lambda_{\min}}^{\lambda_{\max}} I^{\mathrm{Q}}(\lambda)\mathrm{d}\lambda}. \tag{6b}$$

Spectral sensitivity of the ideal quantum sensor $\varepsilon^{Q}_{idQ}(\lambda)$ is constant over the spectral interval of the measured radiation $I^{Q}(\lambda)$

$$\varepsilon^{Q}_{idQ}(\lambda) = \mu_Q = \text{const.} \tag{4a}$$

The relative spectral sensitivity of the quantum sensor is defined as

$$\bar{\varepsilon}^{Q}_{Q}(\lambda) = \frac{\varepsilon^{Q}_{Q}(\lambda)}{\varepsilon^{Q}_{idQ}(\lambda)} = \frac{\varepsilon^{Q}_{Q}(\lambda)}{\mu_Q}. \tag{8a}$$

Following Eqs. (5b) and (8a) the integral output of the quantum sensor in measuring the irradiance $I^{Q}(\lambda)$ is

$$n_Q = \mu_Q \int_{\lambda_{min}}^{\lambda_{max}} \bar{\varepsilon}^{Q}_{Q}(\lambda) I^{Q}(\lambda) d\lambda \tag{5c}$$

and its integral sensitivity

$$\varepsilon^{Q}_{Q} = \frac{n_Q}{I^{Q}} = \frac{\mu_Q \int_{\lambda_{min}}^{\lambda_{max}} \bar{\varepsilon}^{Q}_{Q}(\lambda) I^{Q}(\lambda) d\lambda}{I^{Q}}. \tag{6c}$$

It should be emphasized here that Eq. (8a) determines the relative spectral sensitivity of the quantum sensor in respect of the ideal quantum sensor. Usually, relative spectral sensitivity is determined relative to the ideal energy sensor. Taking into account that for a certain sensor, spectral output does not depend on the units selected to describe the spectral irradiance $I(\lambda)$, one can write, following Eqs. (1) and (3a), for the quantum sensor

$$\begin{aligned} n_Q(\lambda) &= \varepsilon^{Q}_{Q}(\lambda) I^{Q}(\lambda) = \varepsilon^{Q}_{Q}(\lambda) \frac{\lambda}{\gamma} I^{E}(\lambda) \\ &= \varepsilon^{E}_{Q}(\lambda) I^{E}(\lambda), \end{aligned} \tag{10}$$

where $\varepsilon^{E}_{Q}(\lambda) = (\lambda/\gamma)\varepsilon^{Q}_{Q}(\lambda)$ is the spectral sensitivity of the quantum sensor in energy units. The integral sensitivity of the quantum sensor in energy units is

$$\begin{aligned} \varepsilon^{E}_{Q} &= \frac{\int_{\lambda_{min}}^{\lambda_{max}} \varepsilon^{Q}_{Q}(\lambda) \frac{\lambda}{\gamma} I^{E}(\lambda) d\lambda}{I^{E}} \\ &= \frac{\mu_Q \int_{\lambda_{min}}^{\lambda_{max}} \bar{\varepsilon}^{Q}_{Q}(\lambda) \frac{\lambda}{\gamma} I^{E}(\lambda) d\lambda}{I^{E}} \\ &= \frac{\mu_E \int_{\lambda_{min}}^{\lambda_{max}} \bar{\varepsilon}^{E}_{Q}(\lambda) I^{E}(\lambda) d\lambda}{I^{E}}, \end{aligned} \tag{11}$$

where

$$\bar{\varepsilon}^{E}_{Q}(\lambda) = \frac{\mu_Q \lambda \bar{\varepsilon}^{Q}_{Q}(\lambda)}{\mu_E \gamma} \tag{8b}$$

is the relative spectral sensitivity of the quantum sensor as determined relative to the ideal energy sensor.

For the ideal quantum sensor $\bar{\varepsilon}^{E}_{idQ}(\lambda) = \mu_Q \lambda / \mu_E \gamma$ and

$$\varepsilon^{E}_{idQ} = \frac{\mu_Q \int_{\lambda_{min}}^{\lambda_{max}} \frac{\lambda}{\gamma} I^{E}(\lambda) d\lambda}{I^{E}}. \tag{12}$$

From Eqs. (11) and (12) it follows that the relative spectral sensitivity of the ideal quantum sensor relative to the ideal energy sensor is proportional to wave length, and integral sensitivity depends on the spectral composition of the measured radiation. Therefore, comparison of the ideal energy and quantum sensors is possible only when they are calibrated using the same light source.

It should be mentioned here that relative spectral sensitivities are usually normalized in some way for better collation of different sensors. As a rule, the normalizing condition is that $\max[\bar{\varepsilon}(\lambda)] \equiv 1$ or $\bar{\varepsilon}(\lambda) \equiv 1$ at a certain wave length λ. Below, normalizing constants will not be indicated in formulae, because, since our ultimate interest is to find out relative corrections or relations, the constants are cancelled out.

3. Photosynthetically active radiation

As we noted earlier, PAR is not unanimously defined. Accepting the nowadays more commonly used spectral interval from 400 to 700 nm, we will consider PAR in parallel following two possible definitions. PAR as integral energy irradiance within the mentioned spectral limits is denoted as PARE, while PAR as integral quantum irradiance within the same limits is designated as PARQ. Both can be expressed in energy or quantum units, which is marked with the superscript indexes E and Q, respectively. Hence, integral energy PARE in energy units is

$$I^{E}_{PARE} = \int_{400}^{700} I^{E}(\lambda) d\lambda \tag{2d}$$

and in quantum units

$$I^{\mathrm{Q}}_{\mathrm{PARE}} = \frac{1}{\gamma}\int_{400}^{700} \lambda I^{\mathrm{E}}(\lambda)\mathrm{d}\lambda. \tag{2e}$$

Integral quantum PARQ in quantum units is

$$I^{\mathrm{Q}}_{\mathrm{PARQ}} = \int_{400}^{700} I^{\mathrm{Q}}(\lambda)\mathrm{d}\lambda \tag{2f}$$

and in energy units

$$I^{\mathrm{E}}_{\mathrm{PARQ}} = \gamma\int_{400}^{700} \frac{I^{\mathrm{Q}}(\lambda)}{\lambda}\mathrm{d}\lambda. \tag{2g}$$

All the above conclusions and relations regarding the energy and quantum treatments of radiation are valid also for PAR in the cases where the PAR spectral region and the spectral sensitivity of PAR sensors are taken into account.

Thus one can define the ideal PAR energy sensor as a sensor which measures spectral irradiance $I^{\mathrm{E}}(\lambda)$ nonselectively in spectral region from 400 to 700 nm and is not sensitive at all outside this region, i.e. $\varepsilon^{\mathrm{E}}_{\mathrm{idPARE}}(\lambda) \equiv \mathrm{const} = \mu_{\mathrm{E}}$ when $400 \le \lambda \le 700$ nm, and $\varepsilon^{\mathrm{E}}_{\mathrm{idPARE}}(\lambda) \equiv 0$ when $\lambda < 400$ nm or $\lambda > 700$ nm. When measuring spectral irradiance in quantum units $I^{\mathrm{Q}}(\lambda)$ the spectral sensitivity of the ideal PAR energy sensor is $\varepsilon^{\mathrm{Q}}_{\mathrm{idPARE}}(\lambda) = \mu_{\mathrm{E}}\gamma/\lambda$ within the spectral limits shown above.

The spectral sensitivity of the ideal PAR quantum sensor $\varepsilon^{\mathrm{Q}}_{\mathrm{idPARQ}}(\lambda) \equiv \mathrm{const} = \mu_{\mathrm{Q}}$ at $400 \le \lambda \le 700$ nm, and $\varepsilon^{\mathrm{Q}}_{\mathrm{idPARQ}}(\lambda) \equiv 0$ at $\lambda < 400$ nm or $\lambda > 700$ nm, when irradiance is expressed in quantum units. When irradiance is expressed in energy units then $\varepsilon^{\mathrm{E}}_{\mathrm{idPARQ}}(\lambda) = \mu_{\mathrm{Q}}\lambda/\gamma$.

When the same spectral irradiance is measured using different ideal PAR sensors (ideal PAR energy sensor or ideal PAR quantum sensor) the result will also be different.

$$n_{\mathrm{idPARE}} = \mu_{\mathrm{E}}\int_{400}^{700} I^{\mathrm{E}}(\lambda)\mathrm{d}\lambda = \mu_{\mathrm{E}}\gamma\int_{400}^{700} \frac{I^{\mathrm{Q}}(\lambda)}{\lambda}\mathrm{d}\lambda \tag{3b}$$

$$n_{\mathrm{idPARQ}} = \mu_{\mathrm{Q}}\int_{400}^{700} I^{\mathrm{Q}}(\lambda)\mathrm{d}\lambda = \frac{\mu_{\mathrm{Q}}}{\gamma}\int_{400}^{700} \lambda I^{\mathrm{E}}(\lambda)\mathrm{d}\lambda \tag{3c}$$

From Eqs. (3b) and (3c) it is possible to draw two important conclusions:

(1) The relation between integral PARE and PARQ, measured according to different definitions of PAR, using ideal PAR energy and ideal PAR quantum sensors

$$\frac{I_{\mathrm{idPARE}}}{I_{\mathrm{idPARQ}}} = \frac{\gamma\mu_{\mathrm{E}}}{\mu_{\mathrm{Q}}}\frac{\int_{400}^{700} I^{\mathrm{E}}(\lambda)\mathrm{d}\lambda}{\int_{400}^{700}\lambda I^{\mathrm{E}}(\lambda)\mathrm{d}\lambda} = \frac{\gamma\mu_{\mathrm{E}}}{\mu_{\mathrm{Q}}}\frac{\int_{400}^{700}(I^{\mathrm{Q}}(\lambda)/\lambda)\mathrm{d}\lambda}{\int_{400}^{700} I^{\mathrm{Q}}(\lambda)\mathrm{d}\lambda} \tag{13}$$

is not constant; but depends on the spectral composition of the measured radiation.

(2) The product $\mu_{\mathrm{E}}\gamma/\lambda$ in Eq. (3b) can be considered the spectral sensitivity of the ideal PAR energy sensor when the measured spectral irradiance is expressed in quantum units. The relative spectral sensitivity of the ideal PAR energy sensor, determined relative to the ideal quantum sensor, is in this case $\bar{\varepsilon}^{\mathrm{Q}}_{\mathrm{idPARE}} = \mu_{\mathrm{E}}\gamma/\mu_{\mathrm{Q}}\lambda$. For the ideal PAR quantum sensor $\bar{\varepsilon}^{\mathrm{Q}}_{\mathrm{idPARQ}} \equiv 1$. Analogously, the relative spectral sensitivity of the ideal PAR quantum sensor relative to the ideal energy sensor, when measuring spectral irradiance in energy units, is $\bar{\varepsilon}^{\mathrm{E}}_{\mathrm{idPARQ}}(\lambda) = \mu_{\mathrm{Q}}\lambda/\mu_{\mathrm{E}}\gamma$. The spectral properties of the real PAR sensor are characterized by its spectral sensitivity $\varepsilon(\lambda)$ which can be expressed both in energy and quantum units. The electrical output of the real sensor is

$$n(\lambda) = \varepsilon^{\mathrm{E}}(\lambda)I^{\mathrm{E}}(\lambda) = \frac{\varepsilon^{\mathrm{E}}(\lambda)\gamma I^{\mathrm{Q}}(\lambda)}{\lambda} = \varepsilon^{\mathrm{Q}}(\lambda)I^{\mathrm{Q}}(\lambda) \tag{3d}$$

Here the product $\varepsilon^{\mathrm{Q}}(\lambda) = \varepsilon^{\mathrm{E}}(\lambda)\gamma/\lambda$ is the spectral sensitivity of the real PAR sensor in quantum units. The relative spectral sensitivity of the real PAR sensor relative to the ideal energy sensor is $\bar{\varepsilon}^{\mathrm{E}}(\lambda) = \varepsilon^{\mathrm{E}}(\lambda)/\mu_{\mathrm{E}}$, while relative to the ideal quantum sensor is $\bar{\varepsilon}^{\mathrm{Q}}(\lambda) = \varepsilon^{\mathrm{Q}}(\lambda)/\mu_{\mathrm{Q}} = \varepsilon^{\mathrm{E}}(\lambda)\gamma/\lambda\mu_{\mathrm{Q}}$.

Both integral radiation and PAR can be expressed in energy as well in quantum units irrespective of the definition or the type of sensor used in measurement Combining Eqs. (1), (2a), (2b), (2d), (2e), (2f) and (2g) yields

$$U^{\mathrm{I}} = \frac{I^{\mathrm{E}}}{I^{\mathrm{Q}}} = \gamma \frac{\int_{\lambda_{\min}}^{\lambda_{\max}} I^{\mathrm{E}}(\lambda)\mathrm{d}\lambda}{\int_{\lambda_{\min}}^{\lambda_{\max}} \lambda I^{\mathrm{E}}(\lambda)\mathrm{d}\lambda} = \gamma \frac{\int_{\lambda_{\min}}^{\lambda_{\max}} (I^{\mathrm{Q}}(\lambda)/\lambda)\mathrm{d}\lambda}{\int_{\lambda_{\min}}^{\lambda_{\max}} I^{\mathrm{Q}}(\lambda)\mathrm{d}\lambda} \quad (14)$$

$$U^{\mathrm{I}}_{\mathrm{PAR}} = \frac{I^{\mathrm{E}}_{\mathrm{PAR}}}{I^{\mathrm{Q}}_{\mathrm{PAR}}} = \gamma \frac{\int_{400}^{700} I^{\mathrm{E}}(\lambda)\mathrm{d}\lambda}{\int_{400}^{700} \lambda I^{\mathrm{E}}(\lambda)\mathrm{d}\lambda} = \gamma \frac{\int_{400}^{700} (I^{\mathrm{Q}}(\lambda)/\lambda)\mathrm{d}\lambda}{\int_{400}^{700} I^{\mathrm{Q}}(\lambda)\mathrm{d}\lambda} \quad (14a)$$

The conversion factors U^{I} and $U^{\mathrm{I}}_{\mathrm{PAR}}$ for different kinds of radiation are presented in Table 4. An important radiation characteristic in biogeophysical studies is the ratio of PAR to the integral radiation K^{I} which can be expressed as

$$K^{\mathrm{I}} = \frac{I^{\mathrm{E}}_{\mathrm{PAR}}}{I^{\mathrm{E}}_{\mathrm{E}}}. \quad (15)$$

Evidently, as a result of the wider application of PAR quantum sensors, another characteristic, PAR quantum efficiency χ^{I} , has been lately taken into use. It is defined as

$$\chi^{\mathrm{I}} = \frac{I^{\mathrm{Q}}_{\mathrm{PAR}}}{I^{\mathrm{E}}_{\mathrm{E}}}. \quad (16)$$

K^{I} and χ^{I} are calculated for different sensors and for different kinds of radiation.

4. Spectral corrections

All real sensors for integral radiation as well for PAR differ from ideal ones in that their spectral interval of sensitivity does not correspond to that of the ideal sensor and also in that they are more or less selective within their spectral band (Figs. 1 and 2). These deviations cause systematic errors which are usually called spectral errors. Spectral errors depend on the spectral sensitivity of the sensor $\varepsilon(\lambda)$, the spectral composition of the measured irradiance $I(\lambda)$ and the spectral composition of radiation used to calibrate the sensor. It should be emphasized that for correct determination of spectral corrections, the spectral sensitivity of each individual sensor as well as the spectral composition of radiation in case of a certain measurement must be known. Practically, we know the averaged relative spectral sensitivity for a certain class of sensors and spectral irradiance of different kinds of radiation under typical conditions. Hence all spectral corrections are only approximate depending on how much the real situation differs from the expected one.

4.1. Sensors for integral solar radiation

The ideal energy sensor of integral solar radiation must be nonselective in a wide spectral region of solar radiation, practically from 300 to 2500 nm. Sensors with unprotected black receiving surfaces (pyrheliometers, actinometers) are very close to ideal ones. While thermoelectrical pyranometers with glass domes also satisfy these conditions quite well, the instruments based on silicon photocells such as the LI-COR LI-200SA Pyranometer Sensor differ significantly from ideal sensors.

Usually, pyranometers are calibrated relative to pyrheliometers or actinometers, which can be regarded as ideal sensors, using direct solar radiation. In this case Eq. (9) can be used to calculate spectral corrections for different kinds of radiation

$$\beta^{\mathrm{I}}_{\mathrm{PYR}} = \frac{\int_{\lambda_{\min}}^{\lambda_{\max}} \bar{\varepsilon}_{\mathrm{PYR}}(\lambda) I^{\mathrm{E}}(\lambda)\mathrm{d}\lambda}{I^{\mathrm{E}}}, \quad (9a)$$

where $I^{\mathrm{E}}(\lambda)$ is direct solar, global, diffuse or reflected spectral irradiance.

When the pyranometer is calibrated relative to the reference pyranometer using global radiation $G^{\mathrm{E}}(\lambda)$ spectral corrections have to be calculated as

$$\beta^{\mathrm{I}}_{\mathrm{PYR}} = \frac{\int_{\lambda_{\min}}^{\lambda_{\max}} \bar{\varepsilon}_{\mathrm{PYR}}(\lambda) G^{\mathrm{E}}(\lambda)\mathrm{d}\lambda \int_{\lambda_{\min}}^{\lambda_{\max}} \bar{\varepsilon}_{\mathrm{REF}}(\lambda) I^{\mathrm{E}}(\lambda)\mathrm{d}\lambda}{\int_{\lambda_{\min}}^{\lambda_{\max}} \bar{\varepsilon}_{\mathrm{REF}}(\lambda) G^{\mathrm{E}}(\lambda)\mathrm{d}\lambda \int_{\lambda_{\min}}^{\lambda_{\max}} \bar{\varepsilon}_{\mathrm{PYR}}(\lambda) I^{\mathrm{E}}(\lambda)\mathrm{d}\lambda}, \quad (9b)$$

where $\bar{\varepsilon}(\lambda)_{\mathrm{REF}}$ is the relative spectral sensitivity of the reference pyranometer and $\bar{\varepsilon}(\lambda)_{\mathrm{PYR}}$ is the relative spectral sensitivity of the pyranometer to be calibrated; $I^{\mathrm{E}}(\lambda)$ is direct solar, diffuse or reflected spectral irradiance.

Spectral corrections $\beta^{\mathrm{I}}_{\mathrm{PYR}}$ for a typical pyranometer and for the LI-COR LI-200SA Pyranometer Sensor, calculated according to Eq. (9a) and Eq. (9b), are

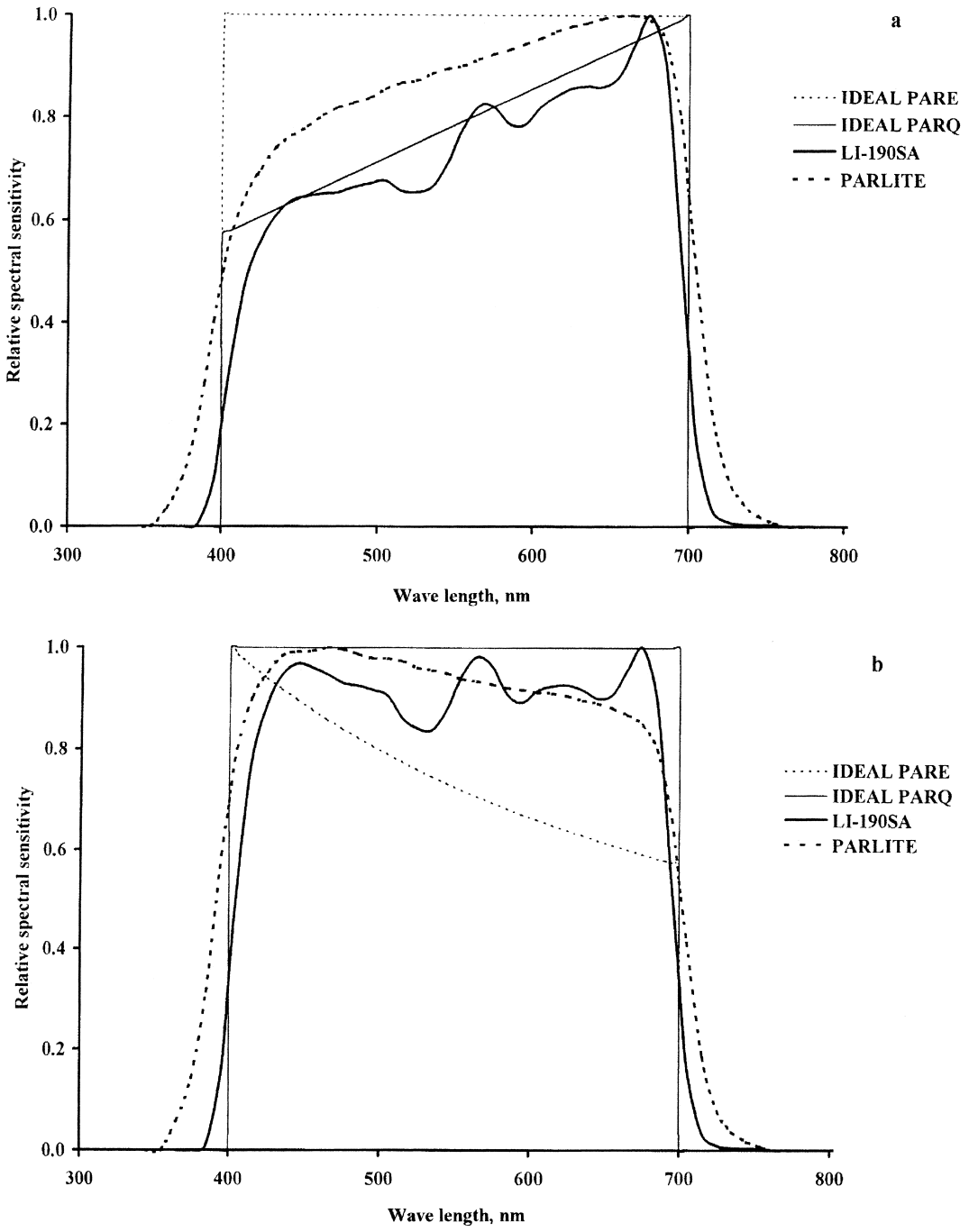

Fig. 1. Relative spectral sensitivity of PAR sensors: (a) relative to the ideal energy sensor, (b) relative to the ideal quantum sensor.

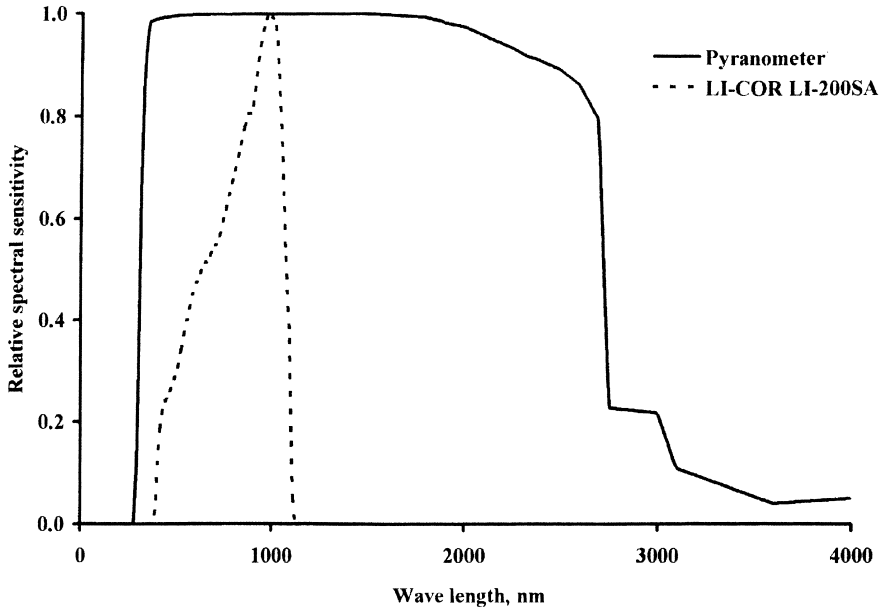

Fig. 2. Relative spectral sensitivity of integral energy sensors relative to the ideal energy sensor.

presented in Table 1. It is evident that a typical pyranometer with a black receiving surface and double glass domes is very close to the ideal energy sensor. It should be noted here that spectral corrections for pyranometers with a black-and-white receiving surface such as Yanishevsky's pyranometer are considerably larger (Ross, 1957).

4.2. PAR sensors

Due to technical problems, the relative spectral sensitivity of real PAR sensors is an approximation to the relative spectral sensitivity of the ideal PAR sensor (Fig.1). For a real sensor $\bar{\varepsilon}_{\mathrm{PAR}}(\lambda) \neq \bar{\varepsilon}_{\mathrm{idPAR}}(\lambda)$, so errors will occur. Spectral corrections of the real PAR sensor can be calculated relative to the ideal PAR energy or ideal PAR quantum sensors. As the real PAR sensors under consideration (LI-COR LI-190SA Quantum Sensor and Kipp and Zonen PAR LITE (1999)) are closer to the ideal PAR quantum sensor, the spectral corrections presented in Eq. (9c) are calculated relative to the ideal PAR quantum sensor. The ratio of the output of the real sensor to that of the ideal PAR quantum sensor, $\beta^{\mathrm{I}}_{\mathrm{PAR}}$, is

$$\beta^{\mathrm{I}}_{\mathrm{PAR}} = \frac{n_{\mathrm{PAR}}}{n_{\mathrm{idPARQ}}} = \frac{\int_{\lambda_{\min}}^{\lambda_{\max}} \bar{\varepsilon}^{\mathrm{E}}_{\mathrm{PAR}}(\lambda) I^{\mathrm{E}}(\lambda)\mathrm{d}\lambda}{\int_{400}^{700} \bar{\varepsilon}^{\mathrm{E}}_{\mathrm{idPARQ}}(\lambda) I^{\mathrm{E}}(\lambda)\mathrm{d}\lambda} = \delta_1 + \delta_2 + \delta_3, \quad (9c)$$

where

$$\delta_1 = \frac{\int_{\lambda_{\min}}^{\lambda_{400}} \bar{\varepsilon}^{\mathrm{E}}_{\mathrm{PAR}}(\lambda) I^{\mathrm{E}}(\lambda)\mathrm{d}\lambda}{\int_{400}^{700} \bar{\varepsilon}^{\mathrm{E}}_{\mathrm{idPARQ}}(\lambda) I^{\mathrm{E}}(\lambda)\mathrm{d}\lambda},$$

Table 1
Spectral correction factors β^{I} (Eqs. (9a) and (9b)) for the typical pyranometer calibrated relative to the normal pyrheliometer and for the LI-COR LI-200SA Pyranometer Sensor calibrated relative to the reference pyranometer for different kinds of radiation

Radiation	Pyranometer		LI-200SA	
	Clear	Overcast	Clear	Overcast
Direct *S*	1.000	–	1.010	–
Diffuse *D*	1.000	–	0.950	–
Global *G*	0.999	0.994	1.000	0.996
Penetrated global				
LAI = 1.8	1.005	1.002	1.115	1.131
LAI = 5.0	1.007	1.006	1.216	1.253
Rainforest	1.006	1.004	1.118	1.159
Reflected global *R*	1.009	1.008	1.419	1.440

$$\delta_2 = \frac{\int_{700}^{\lambda_{max}} \bar{\varepsilon}^{E}_{PAR}(\lambda) I^{E}(\lambda) d\lambda}{\int_{400}^{700} \bar{\varepsilon}^{E}_{idPARQ}(\lambda) I^{E}(\lambda) d\lambda},$$

and

$$\delta_3 = \frac{\int_{400}^{700} \bar{\varepsilon}^{E}_{PAR}(\lambda) I^{E}(\lambda) d\lambda}{\int_{400}^{700} \bar{\varepsilon}^{E}_{idPARQ}(\lambda) I^{E}(\lambda) d\lambda}.$$

The ratio β^{I}_{PAR} can be considered as the correction of the integral sensitivity of the real PAR quantum sensor relative to the ideal one when measuring the spectral irradiance $I^{E}(\lambda)$. The parameter δ_1 characterizes the error caused by the 'parasitic' sensitivity of the real sensor in the spectral interval $\lambda_{min} < \lambda < 400$ and δ_2 characterizes the same type of error in the interval $700 < \lambda < \lambda_{max}$.The addend δ_3 describes the error caused by the deviation of the relative spectral sensitivity of the real PAR sensor from that of the ideal sensor within the PAR spectral region $400 \leq \lambda \leq 700$ nm. When one knows β^{I}_{PAR} and its components for different kinds of radiation it is possible to estimate how close the real sensor is to the ideal PAR quantum sensor and how the deviations of the measured values from PAR depend on the spectral composition of radiation (Table 2).

PAR sensors are usually calibrated by manufacturers using standard lamps with a known spectral irradiance $I^{E}_{L}(\lambda)$. In this case integral sensitivity is

$$\varepsilon^{L}_{PAR} = \frac{\mu_E \int_{\lambda_{min}}^{\lambda_{max}} \bar{\varepsilon}^{E}_{PAR}(\lambda) I^{E}_{L}(\lambda) d\lambda}{\int_{400}^{700} I^{E}_{L}(\lambda) d\lambda}. \quad (6d)$$

When measuring the spectral irradiance $I^{E}(\lambda)$ whose spectral composition differs from $I^{E}_{L}(\lambda)$, the integral sensitivity appears different. To eliminate this difference, the spectral correction, $\beta^{I}(\lambda)$, has to be calculated as

$$\beta^{I}_{PAR} = \frac{\varepsilon^{I}_{PAR}}{\varepsilon^{L}_{PAR}} = \frac{\int_{\lambda_{min}}^{\lambda_{max}} \bar{\varepsilon}^{E}_{PAR}(\lambda) I^{E}(\lambda) d\lambda \int_{400}^{700} \bar{\varepsilon}^{E}_{idPARQ} I^{E}_{L}(\lambda) d\lambda}{\int_{\lambda_{min}}^{\lambda_{max}} \bar{\varepsilon}^{E}_{PAR}(\lambda) I^{E}_{L}(\lambda) d\lambda \int_{400}^{700} \bar{\varepsilon}^{E}_{idPARQ} I^{E}(\lambda) d\lambda}. \quad (9d)$$

Substituting in Eq. (9d) $S(\lambda)$, $G(\lambda)$, $R(\lambda)$ etc. for $I^{E}(\lambda)$ one can calculate spectral corrections for different

Table 2
Spectral correction factors β_{PAR} (Eq. (9b)) of PAR sensors due to the deviation of their spectral sensitivity from that of the ideal PAR quantum sensor. The sensors are calibrated relative to the LI-COR calibration lamp

Radiation	LI-COR LI-190SA				Kipp and Zonen PAR LITE			
	β_{PAR}	δ_1	δ_2	δ_3	β_{PAR}	δ_1	δ_2	δ_3
Clear sky								
Global *G*	0.996	0.002	0.986	0.008	1.010	0.016	0.967	0.027
Direct *S*	0.998	0.003	0.986	0.009	1.007	0.013	0.965	0.029
Diffuse *D*	0.992	0.004	0.982	0.006	1.023	0.027	0.976	0.020
Reflected *R*	0.995	0.001	0.961	0.033	1.058	0.006	0.936	0.116
Penetrated								
LAI = 1.8	0.996	0.003	0.983	0.010	1.031	0.022	0.975	0.034
LAI = 5.0	1.009	0.003	0.986	0.020	1.075	0.018	0.972	0.085
Rainforest	0.999	0.003	0.983	0.013	1.032	0.015	0.966	0.051
Overcast								
Global *Q*	0.996	0.003	0.985	0.008	1.013	0.018	0.968	0.027
Reflected *R*	0.994	0.001	0.959	0.034	1.059	0.006	0.935	0.118
Penetrated								
LAI = 1.8	0.996	0.004	0.982	0.010	1.035	0.025	0.975	0.035
LAI = 5.0	1.008	0.004	0.984	0.020	1.079	0.021	0.973	0.085
Rainforest	0.999	0.003	0.983	0.013	1.035	0.017	0.966	0.052
Calibration lamp								
LI-COR	1.000	0.001	0.982	0.017	1.000	0.004	0.937	0.059
Kipp and Zonen	1.000	0.001	0.980	0.019	1.000	0.003	0.933	0.064

kinds of radiation for the real PAR quantum sensor calibrated relative to the standard lamp (Table 2).

5. Spectral composition of radiation above and inside vegetation canopies

As discussed earlier, to calculate different corrections and conversion factors, data on the spectral distribution of radiation over the whole spectrum are needed. However, the data obtained from model calculations or measurements with different types of spectroradiometers and under different atmospheric conditions are unsystematic and of variable quality.

Using the standard model of the cloudless atmosphere Avaste et al. (1962) calculated the spectral distribution of the direct solar radiation $S(\lambda)$ and diffuse radiation $D(\lambda)$ in mcal cm^{-2} min^{-1} (0.699 W m^{-2}) at sea level for different relative air mass m, turbidity τ and water vapour content ω. The calculations were performed for the whole spectral region of solar radiation 290–4000 nm. Bird and colleagues (Bird et al., 1982, 1983; Bird, 1984; Bird and Riordan, 1986) presented the spectral distribution (W m^{-2} nm^{-1}) of direct $S(\lambda)$, diffuse $D(\lambda)$ and global solar radiation $G(\lambda) = S(\lambda) \sin h + D(\lambda)$ and diffuse radiation of the cloudy sky $D_C(\lambda)$. The calculations were performed for the spectral interval 305–2450 nm using the models BRITE and SPECTRAL. Comparison of model calculations with data obtained from measurements by spectroradiometers have shown fairly good agreement.

Czarnowski (1994a, b) and Czarnowski and Cebula (1996) performed a number of spectral irradiance measurements of incoming global, direct and diffuse radiation in the spectral interval 300–1100 nm using the LI-1800 spectroradiometer. They also measured global radiation above and inside tomato and green pepper crops in the greenhouse at different leaf area indexes.

Endler (1993) studied the spectral radiance and irradiance of penetrated radiation in the PAR spectral region above and inside a riparian forest and discussed the influence of the spectral composition of PAR on plant growth.

Using the LI-1800 spectroradiometer Ross et al. (1986) studied $G^Q(\lambda)$ and red/far-red ratio in the understorey of boreal forest ecosystems in the spectral region 400–800 nm. Kylling (1993) calculated $D_C^E(\lambda)$ in the interval 300–800 nm for the cloudy sub-arctic summer atmosphere at $h = 30^\circ$, studied the influence of albedo on $D_C^E(\lambda)$ and found that presence of water clouds generally reduces $D_C^E(\lambda)$.

Spectral transmittance of solar radiation through a dense canopy is low, especially in the PAR region. Using the LI-COR spectroradiometer LI-1800, Lee (1987) measured $G(\lambda)$ between 300 and 1100 nm of a Costa Rica rainforest at solar elevation near the zenith. In the PAR region the transmittance $T(\lambda)$ is as low as about 0.5%, while in the near infrared (NIR) region it is about 4%. The height of the forest was 35 m, and although LAI was not given, such low transmittance indicates that it must have been about 10.

Similar results were obtained by Lee and Downum (1991) in Miami, Florida, where the spectroradiometer LI-1800 was also used.

The measurements made by Ross at al. (1986) in a *Picea glauca* forest (Alberta, Canada) using identical instruments, with the height of trees being 32 m, showed that PAR transmittance there was about 2–3% and NIR transmittance about 5%, i.e. 4–5 times higher than in the rainforest. Unfortunately, LAI was not known. The spectral distribution of the global radiation $G(\lambda)$ in the interval 400–800 nm was measured in the open area ($G_0(\lambda)$) and beneath the forest ($G_T(\lambda)$) at a height of 1 m. Using these data we calculated the spectral transmittance $T(\lambda)$ as the ratio $G_T(\lambda)/G_0(\lambda)$.

The spectral transmittance $T(\lambda)$ in the spectral interval 380–1550 nm of maize, sorghum, soybean and sunflower in a Mediterranean climate of Western Australia was measured by Bishnoi and Sedgley (1985). They used a portable ISCO spectroradiometer with a flat sensor 2 cm in diameter, fitted with a fibre optic extension cord. The results showed that in the PAR region $T(\lambda)$ varied between 3 and 8%. In the NIR region variation was larger, $T(\lambda)$ being between 15 and 35%. LAI of different crops ranges from 3.5 to 5.5. With increasing LAI, penetration decreases sharply in maize and sorghum crops which have an open foliage. Decrease is slower in a clustered foliage like that of soybean and cowpea. The authors concluded that the parameters of transmitted radiation and crop geometry are strongly interdependent and regulate radiation transmission through the foliage.

Scott et al. (1968) measured the global radiation transmitted and reflected by 16 contrasting types of vegetation. They used a portable spectroradiometer which had near-cosine response and covered the spec-

tral range 400–1050 nm. Transmission measurements were made using a fibre optic extension cord with a flat receiving surface of 2 cm in diameter, while reflection measurements were performed with the angle of acceptance limited to 22°. LAI of the crops varied between 2 and 10.

The most comprehensive studies of spectral reflectance and transmittance at the leaf level were carried out by Jacquemoud and Baret (1990). For calculations, they used the PROSPECT model and for laboratory measurements, the Varian Cary 17DI spectrophotometer equipped with an integrating sphere coated with barium sulphate paint. The accuracy of the measurements was about 1% and agreement with the calculated data appeared very good ($R = 0.98$). The results were published for leaves of green soybean and yellowing maize.

Jacquemoud (1993) calculated canopy reflectance as a function of LAI and leaf and soil optical properties using the hybrid model PROSPECT + SAIL. These calculations show that in the spectral interval 500–1400 nm the canopy reflectance $R(\lambda)$ increases with increasing LAI, while in other spectral intervals this dependence is less pronounced.

For the soybean canopy, analogous calculations with the use of the more simplified model SHORTWAVE were carried out by Lemeur and Rosenberg (1979).

Unfortunately, we have found only a few data (Satterwhite and Henley, 1990; Skidmore and Schmidt, 1998; Turner et al., 1998) for the spectra of green vegetation measured in the whole solar radiation spectral interval 300–2400 nm.

For measurements of spectral reflectance in the spectral region 400–1900 nm, Shibayama and Akiyama (1989) used the field spectroradiometer with the 15° field of view. Optical fibre light cords at 2.5 m above the canopy were used, which limited the sample area to 60 cm in diameter. The measurements were carried out for different rice cultivars at the heading stage. Due to the influence of the water body beneath the crop, the results are somewhat different from the measurements made in 'canopy + soil' system.

Using the spectroradiometer LI-1800 in the spectral interval 400–1100 nm, Lorenzen and Jensen (1991) measured the spectral reflectance of barley crop during the growing season. The results were similar to that of Scott et al. (1968). They found that the growing season can be divided into four district Feekesscale phenological periods on the basis of spectral reflectance .

Using the above data we tried to construct a set of typical spectral curves of direct, diffuse and global incoming solar radiation as well as the radiation reflected and transmitted by the vegetation.

When selecting initial data for estimation of spectral corrections and conversion factors, main attention was given to the reliability of the spectral composition of radiation under different typical conditions; but not to absolute values. As a rule, experimental data were preferred. The choice was to a certain extent subjective and was partially based on the authors' long-term experience. All data were calculated as mean values for 10 nm spectral intervals and these values were allocated to the midpoint of the wave length interval. To cover the spectral region from 300 to 4000 nm different data were combined in some cases, while in the longwave region from 2400 to 4000 nm arbitrary linear extrapolation was used since the energy contribution of this region is negligible.

Spectral irradiance above the canopy (spectral irradiance of the incoming radiation and the radiation reflected from the canopy) is presented in Figs. 3 and 4. For direct solar radiation, data of the spectral irradiance $S(\lambda)$, measured by Bird and Riordan (1986) at Golden (Colorado) at a solar elevation of 69°, were used. These measurements cover the spectral interval from 300 to 2300 nm; linear extrapolation was used starting from the last measured value, i.e. from 2300 to 3010 nm, where $S(\lambda)$ is assumed to be zero. For the clear sky diffuse radiation $D(\lambda)$, the results of the measurements by Endler (1993) were employed. However, since these data cover only the interval 350–700 nm they were combined with the model calculations carried out by Avaste et al. (1962) in the regions 330–350 nm and 700–4000 nm. The spectral irradiance of global radiation was found as the sum $G(\lambda) = S(\lambda)\sin h + D(\lambda)$, where h is solar elevation. For the cloudy sky, global radiation data were taken from Bird et al. (1982); starting from 2300 nm, linear extrapolation was used up to zero at 3100 nm.

Spectral irradiance of the radiation reflected from the vegetation (upward spectral irradiance above the canopy) was calculated by multiplying the global radiation spectral irradiance $G(\lambda)$ by the spectral reflection coefficient (spectral albedo) of the plant cover. For green soybean, spectral reflectance was used mainly

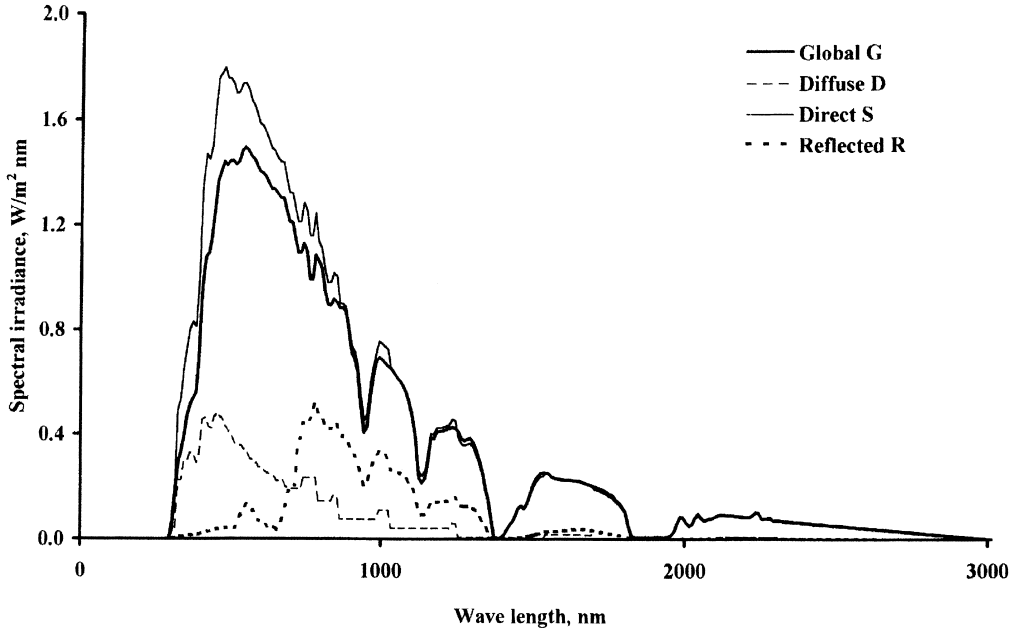

Fig. 3. Typical spectral irradiance above the canopy (clear sky).

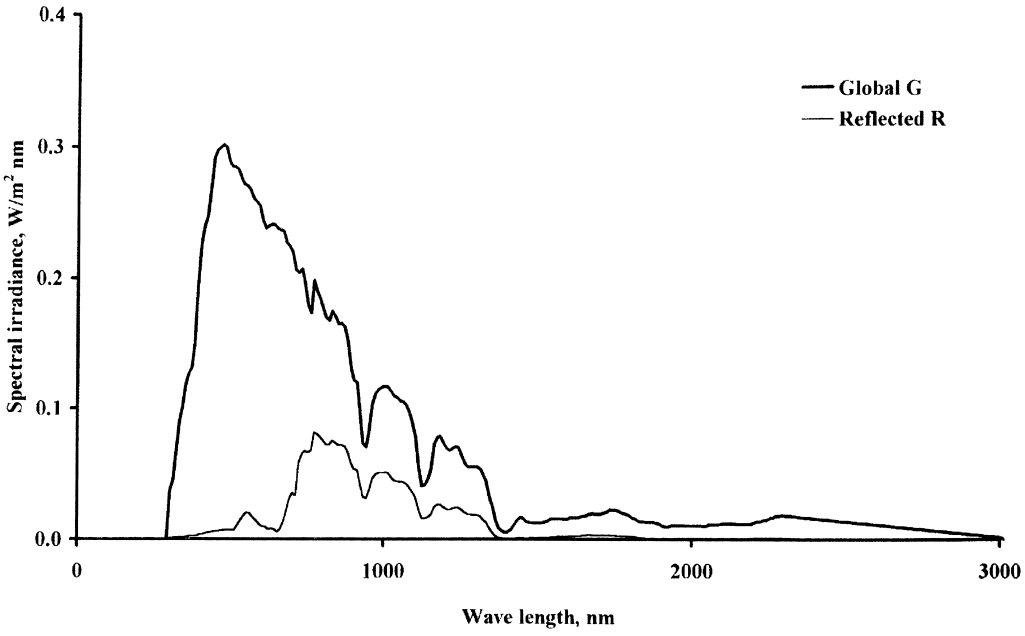

Fig. 4. Typical spectral irradiance above the canopy (overcast).

as in Jacquemoud and Baret (1990), complemented by data from Lemeur and Rosenberg (1979) in the spectral region 300–400 nm and by linear interpolation from 0.021 at 2420 nm to 0.010 at 4000 nm.

Due to the great variability and insufficient amount of reliable experimental data, spectral irradiance inside the plant canopy appears most uncertain. Spectral transmittance for LAI = 1.8 and LAI = 5.0 in the spectral region 350–1100 nm was calculated from the experimental data of spectral irradiance above and inside the plantation (Czarnowski and Cebula, 1996). Since below 350 nm experimental data are unreliable due to technical problems, the constant value equal to spectral transmittance at 340 nm was used in the region 300–340 nm. In the spectral region from 1100 to 2500 nm, the spectral transmittance curve was extended using data from Jacquemoud and Baret (1990) for green soybean leaves, and in the region 2500–4000 nm transmittance was linear decreasing to half. Spectral transmittance was calculated also for deep shade under a rainforest at La Selva, Costa Rica, using experimental data from Lee and Graham (1986). Although LAI was not given, it must have been at least 10 judging by irradiance values. Spectral irradiance inside the canopy was calculated as a product of spectral transmittance and spectral global radiation above the canopy for the clear (Fig. 5) and the overcast sky (Fig. 6).

Since all types of commonly used pyranometers are instruments with double glass domes and a black receiving surface, a typical relative spectral sensitivity of the pyranometer was found using spectral transparency data for domes and spectral reflectance data for black coatings. All known data being similar, we used averaged values. Typical relative spectral sensitivities of the pyranometer and the LI-COR Pyranometer Sensor LI-200SA are presented in Fig. 2. Relative spectral sensitivities of the LI-COR Quantum Sensor LI-190SA and the Kipp and Zonen B. V. PAR LITE sensor (Fig. 1) as well as the spectral irradiance of standard lamps (Fig. 7) were kindly provided by the manufacturers. Spectral irradiance from calibration lamps was extended to longer wave lengths using blackbody radiation at radiation temperature of 3150 K for the LI-COR lamp (estimated) and 2856 K for the Kipp and Zonen lamp (given). In addition, Kipp and Zonen B. V. presented spectral data for the black Kipp paint and the domes used for the CM3, CM6B, CM11 and CM21 pyranometers, which we applied in estimation of the typical spectral sensitivity of pyranometers.

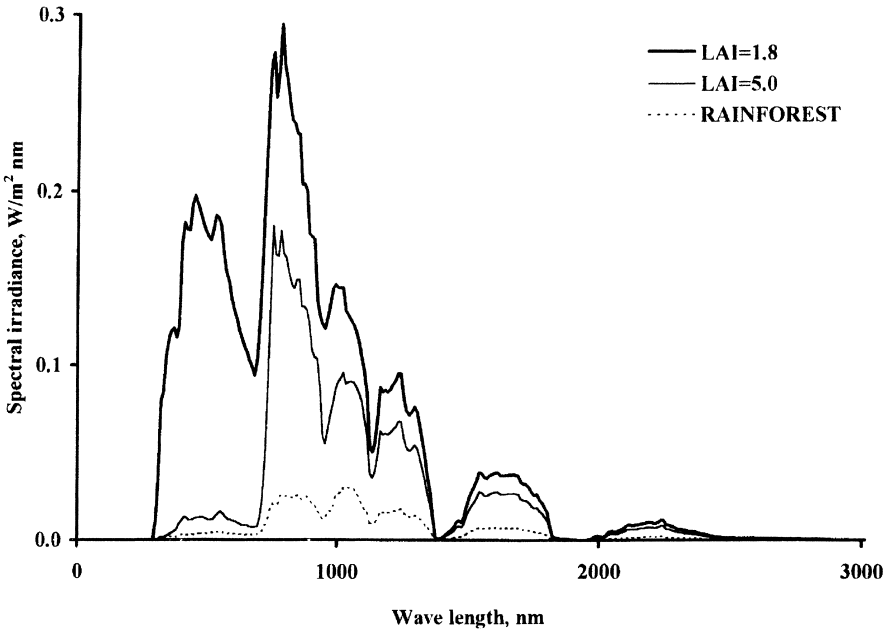

Fig. 5. Typical downward spectral irradiance inside the canopy (clear sky).

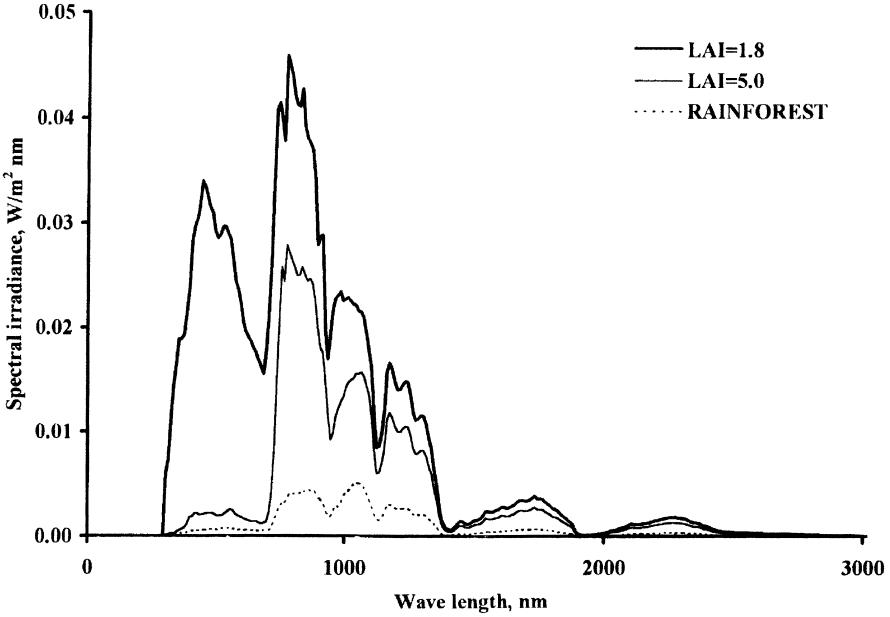

Fig. 6. Typical downward spectral irradiance inside the canopy (overcast).

Relative spectral sensitivities of sensors were normalized so that their maximum value $\max[\bar{\varepsilon}(\lambda)] \equiv 1$.

6. Results of calculations

Table 3 presents the calculated values of the ratio of PAR to the integral radiation K^{I} for different ideal and real sensors. As the LI-COR LI-190SA Quantum Sensor is more widespread and also quite close to the ideal PAR quantum sensor, analysis will be given for this sensor type. It is evident from the Table that the role of PAR in integral radiation is the greatest for clear sky diffuse radiation, but is practically equal for global radiation of clear and the overcast sky. The most significant decrease in the share of PAR takes place inside the plant canopy: in upper canopy layers (LAI = 1.8) the ratio K^{I} decreases about 35%, but in the lower layers of a dense canopy (LAI = 5.0) as much as 8–9 times. The somewhat higher value of K^{I} in the rainforest compared with dense vegetation is presumably caused by the higher degree of clumpiness and by the existence of larger gaps between the trees. Through the gaps one can see a part of the sky with a larger share of diffuse PAR compared with the radiation scattered by leaves. The share of PAR in reflected integral radiation is low ($K^{\mathrm{I}} \approx 0.10$). The share of PAR in the radiation originating from calibration lamps is also low due to their low radiation temperature as compared with the Sun's radiation temperature. In general, PAR efficiency χ^{I} follows the regularities of the ratio K^{I}. The most important conclusion drawn from Table 3 is that the ratio K^{I} decreases rapidly with increasing canopy depth and is low for the radiation reflected from the canopy. Therefore the values of K^{I} estimated for incoming radiation above the canopy are not valid for penetrated or reflected radiation. When PAR is measured with the energy PAR sensor or calculated as energy irradiance between 400 and 700 nm, the ratio K^{I} is 3–12% higher than it is in the cases when PAR is estimated as quantum irradiance.

The conversion factor from quantum units to energy units for PAR $U^{\mathrm{I}}_{\mathrm{PAR}}$ (Table 4) depends on the kind of radiation and is about 40% higher than for integral radiation. The conversion factor of PAR, $U^{\mathrm{I}}_{\mathrm{PAR}}$, is about 6% higher for incoming solar radiation than for reflected radiation.

In the theoretical part we pointed out that when measurement of different kinds of radiation is performed with a pyranometer calibrated relative to a pyrheliome-

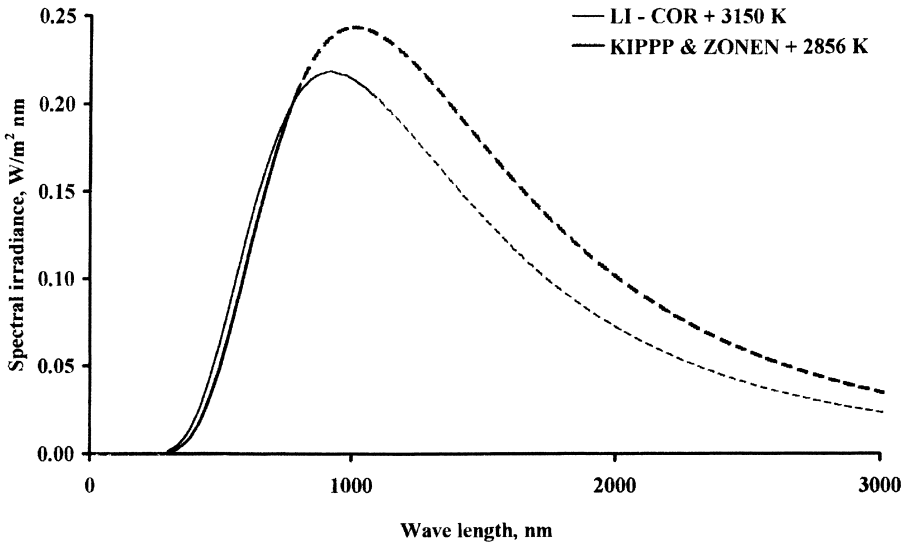

Fig. 7. Spectral irradiance of calibration lamps (dashed lines — blackbody approximation).

ter then a systematic error will occur due to the difference in spectral distribution between direct radiation and the radiation to be measured. Table 1 shows the magnitude of such errors. In case of typical pyranometers, the maximum error is 0.9% when reflected radiation for a cloudless sky is measured. Correction

Table 3
The ratio of photosynthetically active radiation (PAR) to integral radiation K^I (Eq. (15)) and PAR efficiency χ^I (μmol/W s) (Eq. (16)) for PAR ideal energy and PAR ideal quantum sensors and the ratio of PAR, measured with the PAR ideal energy sensor, to PAR measured with the PAR ideal quantum sensor I_{idPARE}/I_{idPARQ} for different kinds of radiation

Radiation	PAR ideal energy sensor		PAR ideal quantum sensor		LI-COR LI-190SA		Kipp & Zonen PAR LITE		I_{idPARE}/I_{idPARQ}
	K^I	χ^I	K^I	χ^I	K^I	χ^I	K^I	χ^I	
Clear sky									
Global *G*	0.434	1.977	0.400	1.821	0.398	1.814	0.404	1.839	1.086
Direct *S*	0.411	1.895	0.382	1.762	0.381	1.758	0.385	1.774	1.075
Diffuse *D*	0.549	2.416	0.487	2.144	0.483	2.127	0.498	2.193	1.127
Reflected *R*	0.099	0.477	0.096	0.464	0.096	0.462	0.102	0.491	1.027
Penetrated global									
LAI = 1.8	0.286	1.274	0.0257	1.144	0.0256	1.139	0.265	1.179	1.114
LAI = 5.0	0.048	0.217	0.044	0.197	0.044	0.199	0.047	0.212	1.102
Rainforest	0.066	0.301	0.061	0.278	0.061	0.278	0.063	0.288	1.080
Overcast sky									
Global *G*	0.434	1.975	0.398	1.814	0.397	1.807	0.403	1.837	1089
Reflected *R*	0.100	0.481	0.097	0.468	0.096	0.465	0.103	0.496	1.028
Penetrated global									
LAI = 1.8	0.292	1.294	0.261	1.158	0.0260	1.154	0.270	1.198	1.117
LAI = 5.0	0.050	0.224	0.045	0.202	0.045	0.204	0.049	0.218	1.105
Rainforest	0.068	0.315	0.062	0.291	0.062	0.290	0.065	0.301	1.083
Calibration lamp									
LI-COR	0.098	0.487	0.098	0.487	0.098	0.487	0.098	0.487	1.000
Kipp & Zonen	0.070	0.348	0.070	0.352	0.070	0.352	0.070	0.352	0.990

Table 4
Conversion factor between integral irradiance in energy and quantum units U^{I} ($W\,s\,\mu mol^{-1}$) (Eq. (14)) and PAR in energy and quantum units U^{I}_{PAR} ($W\,s\,\mu mol^{-1}$) (Eq. (14a)) for different kinds of radiation

Radiation	U^{I}		U^{I}_{PAR}	
	Clear	Overcast	Clear	Overcast
Global G	0.1396	0.1389	0.2195	0.2196
Direct S	0.1350	–	0.2169	–
Diffuse D	0.1845	–	0.2273	–
Reflected R	0.1264	0.1275	0.2072	0.2073
Penetrated global				
LAI = 1.8	0.1381	0.1400	0.2247	0.2254
LAI = 5.0	0.1130	0.1141	0.2223	0.2229
Rainforest	0.1090	0.1102	0.2178	0.2184
Calibration lamp				
LI-COR	0.0819		0.2017	
Kipp and Zonen	0.0765		0.1997	

is practically unnecessary in measurements of incoming solar radiation.

The situation is drastically different when the LI-COR LI-200SA Pyranometer Sensor is used instead of an ordinary pyranometer. The former instrument can be employed for measurement of incoming global radiation only. In measurements of the radiation reflected by the canopy the values can be in error up to 45%, while the values of penetrated radiation can be more than 20% lower.

Table 2 characterises different systematic errors of PAR quantum sensors, caused by deviation of their spectral sensitivity from that of the ideal sensor. One can conclude that for the LI-190SA Quantum Sensor, the errors δ_1 of 'parasitic' sensitivity at $\lambda < 400$ nm are small and do not exceed 0.4%. The errors δ_3 due to 'parasitic' sensitivity at $\delta > 700$ nm are larger, reaching the maximum value of 3.4% in measurements of the radiation reflected by the vegetation. Both errors, δ_1 and δ_2, increase the output of the sensor. More essential are the errors caused by deviation of the relative spectral sensitivity $\bar{\varepsilon}^{E}_{PAR}(\lambda)$ from the ideal $\bar{\varepsilon}^{E}_{idPARQ}(\lambda)$ in the spectral interval $400 \leq \lambda \leq 700$ nm. The magnitude of these errors depends on the kind of radiation to be measured and ranges from 1.4% in measurements of direct solar PAR to 4.9% in measurements of reflected PAR. Since errors δ_1 and δ_3 compensate to some extent for the error δ_2, the total error will be less than 1%.

The situation is somewhat poorer in the case of the Kipp and Zonen PAR LITE quantum sensor. The correction factor δ_1 caused by 'parasitic' sensitivity at $\lambda < 400$ nm varies between 0.6 and 2.7%, being smallest for PAR reflected from the vegetation and largest for clear sky diffuse PAR. The influence of 'parasitic' sensitivity at $\lambda > 700$ nm is greater; δ_3 has a minimum value of 2.0% for clear sky diffuse PAR and a maximum value of 11.8% for PAR reflected from the vegetation under an overcast sky. The δ_2 is considerable (2.4–6.5%) also for downward global radiation inside the canopy. The total correction factor $\beta_{PAR} = \delta_1 + \delta_2 + \delta_3$ is smallest (1.007) for direct solar PAR and largest (1.079) for global overcast sky PAR inside a dense canopy at LAI = 5.0.

It should be noted that the described systematic errors of PAR quantum sensors relative to the ideal PAR quantum sensor are useful to know when analysing the functioning of the sensor and improving the sensor's quality.

7. Concluding remarks

We have found only two papers (McCree, 1972a; Jacovides et al., 1997) where the conversion factor U^{I}_{PAR} (Eq. (14a)) is dealt with. Using the $I(\lambda)$ data of Henderson and Hodgkiss (1963), McCree calculated the conversion factor for two situations: for the clear sky global radiation $U^{G}_{PAR} = 0.219$ and for the clear sky diffuse radiation $U^{D}_{PAR} = 0.236$. The value $U^{G}_{PAR} = 0.219$ has been widely used later by other authors.

Using the spectroradiometer LI-1800 Jacovides et al. (1997) found U^{G}_{PAR} for a polluted atmosphere at Athens to be in the interval 0.219–0.222 depending on atmospheric turbidity. For clear sky diffuse radiation, U^{D}_{PAR} varied from 0.230 to 0.236. While U^{G}_{PAR} decreases with turbidity, U^{D}_{PAR} does not reveal such a tendency. The authors recommend to take $U^{G}_{PAR} = 0.221$ and $U^{D}_{PAR} = 0.234$ as averaged values, which shows very good agreement with our results.

For U^{G}_{PAR}, our calculations (Table 4) yielded the value 0.227 which is 3.7% higher than the result of McCree. For clear sky diffuse radiation, our value $U^{D}_{PAR} = 0.235$ practically coincides with McCree's 0.236. The difference between our values of U^{G}_{PAR} and

Table 5
The relative difference (%) between the conversion factors U^{I}_{PAR} and U^{G}_{PAR}

Sky	U^{G}_{PAR}	U^{S}_{PAR}	U^{D}_{PAR}	U^{T}_{PAR}			U^{R}_{PAR}
				LAI = 1.8	LAI = 5.0	Rainforest	
Clear	0.0	−1.2	+3.6	+2.3	+1.3	−0.8	−5.7
Overcast	0.0	–	–	+2.7	+1.5	−0.5	–5.7

those of McCree is probably caused by the use of different models of $G(\lambda)$ as well by different input optical characteristics of the atmosphere. From Table 4 it follows that U^{G}_{PAR} is not a universal conversion factor but depends on the kind of radiation. The use of the 'universal' conversion factor of McCree, $U^{G}_{PAR} = 0.219$, for some other kinds of radiation could be a source of systematic errors. Table 5 gives the magnitude of errors for different kinds of radiation. The maximum error of −5.7% effects reflected radiation, but the +3.6% error for clear sky diffuse radiation is also appreciable. Unlike errors for the other kinds of radiation the latter is positive in sign, which is caused by the shape of the spectral distribution curve $I(\lambda)$: the maximum of the spectral curve of clear sky diffuse radiation is shifted to shorter wave lengths (see Fig. 1), while for the other kinds of radiation, especially for reflected radiation, the maximum is shifted to longer wave lengths.

To estimate the PAR efficiency χ^{I} (Eq. (16)) different methods have been used. The simplest way is to measure the PAR irradiance I^{Q}_{PARQ} with a PAR quantum sensor, calibrated in quantum units, and the integral irradiance I^{E} with a pyranometer and to find their ratio (Howell et al., 1983; Meek et al., 1984; Alados et al., 1995; Sulev and Ross, 1996). Another way is to calculate I^{Q}_{PARQ} and I^{E}, using the data of spectral irradiance $I(\lambda)$ for different kinds of radiation measured or estimated theoretically on the basis of models. Olseth and Skartveit (1997) applied the sophisticated model SPECTRAL 2 (Bird and Riordan, 1986) for a clear sky and the cloud transmittance model for an overcast sky and calculated χ^{S}, χ^{D}, χ^{G}, χ^{DC} as the functions of the solar elevation h for typical atmospheric conditions at 65°N and at the equator. At $h = 45°$ they obtained $\chi^{S} = 1.85$, $\chi^{D} = 2.50$, $\chi^{G} = 1.95$ and $\chi^{DC} = 2.40$. Comparison of these values and our results (Table 3) shows that agreement is fairly good for χ^{S} and χ^{G}, but χ^{D} is 24% higher than our value for a cloudy sky.

From measurements with the LI-COR quantum sensor, Alados et al. (1995) found that PAR efficiency for the direct solar radiation χ^{S} increases with the solar elevation h from 1.83 at $h = 24°$ to 1.92 at $h = 64°$. This is in good accordance with the value 1.895 calculated by us. For an overcast sky, their measurements yielded $\chi^{G} = 2.1$, which is somewhat higher than our value 1.975. The χ^{G} depends weakly on h, cloud situation and other factors, and its value for a clear midsummer day is 2.00 which is practically the same as the value 1.982 calculated by us.

We measured global PAR G^{Q}_{PAR}, using the LI-COR LI-190SA Quantum Sensor, and the integral global radiation G^{E}, using the Reemann TR-3 pyranometer, in a willow coppice (Ross et al., 1998; Ross and Ross, 1998). Using these data, the PAR quantum efficiency $\chi^{G}(L)$ was calculated as a function of depth within the canopy L (Fig. 8). Both the calculated values and the values of $\chi^{G}(L)$ presented in Table 3 decrease rapidly with L, whereas the experimental values are increased by 10–15%. The reason of this discrepancy is not clear, but it may be caused by various experimental or theoretical faults.

Compared with the PAR efficiency χ^{I} the ratio of PAR to the integral radiation K^{I} is more commonly used. Several data for the ratio K^{I} have been reported in literature. Approximate theoretical estimations of K^{I} as a function of canopy depth were made by Tooming (1967).

The ratio K^{I} can be estimated in different ways:

1. Calculation of K^{I} when the spectral irradiance $I^{E}(\lambda)$ is known (Avaste et al, 1962; McCree, 1976).
2. Simultaneous measurement of I^{E}_{E} and I^{E}_{PAR} using the pyranometer or actinometer with and without broadband filters, respectively (e.g. Tooming and Niilisk, 1967; Stigter and Musabilha, 1982; Blackburn and Proctor, 1983; Rao, 1984; Karalis, 1989; Jacovides et al., 1993; Papaioannou et al., 1996;).
3. Simultaneous measurement of I^{E}_{PAR} with the PAR sensor and I^{E}_{E} with the pyranometer (e.g. Howell et al., 1983; Meek et al., 1984; Weiss and Norman, 1985; Alados et al., 1995; Sulev and Ross, 1996).

In Table 3 the calculated values of the ratio of PAR to integral radiation K^{I} for different kinds of radiation

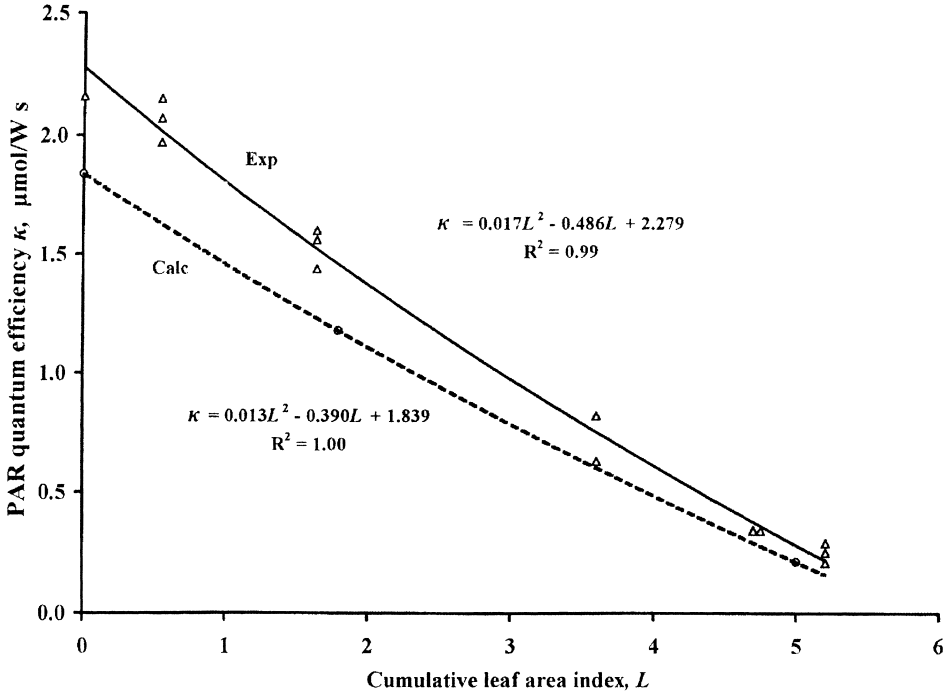

Fig. 8. PAR quantum efficiency χ^{Q} for clear sky global radiation vs cumulative leaf area index L calculated using typical radiation data (Calc) and measured data in a willow coppice (Exp) with trendlines.

are presented. The values are calculated using typical curves of the spectral irradiance $I(\lambda)$. However, experimental data reveal that K^{I} is not constant and depends on a number of environmental factors, for instance, on solar elevation, water content in the atmosphere, atmospheric turbidity, type and amount of clouds, the ratio of diffuse PAR to global PAR, etc. The largest amounts of data are available for the global radiation K^{G} (Papaioannou et al., 1996), which show that K^{G} varies between 0.42 and 0.49. For the cloudy sky diffuse radiation K^{D}, the range of variation is from 0.50 to 0.69, data for the direct solar radiation K^{S} vary between 0.20 and 0.50 and depend primarily on solar elevation.

Both theoretical calculations and experimental data reveal that inside the canopy, the ratio K^{G} for penetrated global radiation depends essentially on canopy depth. Physically, this is influenced by the shape of the spectral curve of leaf absorbtance. In the PAR spectral region green leaves absorb about 85% of radiation, while in the NIR region the respective share is only about 15%. As a result the ratio PAR/NIR decreases rapidly with increasing LAI.

8. List of symbols

G	global radiation (global integral irradiance) ($W\,m^{-2}$)
$G(\lambda)$	spectral global radiation (global spectral irradiance) ($W\,m^{-2}\,nm^{-1}$)
D	diffuse radiation (diffuse integral irradiance) of clear sky ($W\,m^{-2}$)
$D(\lambda)$	spectral diffuse radiation (diffuse spectral irradiance) of clear sky ($W\,m^{-2}\,nm^{-1}$)
D_C	diffuse radiation (diffuse integral irradiance) of overcast sky ($W\,m^{-2}$)
$D_C(\lambda)$	spectral diffuse radiation (diffuse spectral irradiance) of overcast sky ($W\,m^{-2}\,nm^{-1}$)
h	solar elevation (°)
I	integral irradiance (radiant flux density) ($W\,m^{-2}$; $\mu mol\,m^{-2}\,s^{-1}$)

$I(\lambda)$ spectral irradiance ($W\,m^{-2}\,nm^{-1}$; $\mu mol\,m^{-2}\,s^{-1}\,nm^{-1}$)

$I^{E}(\lambda)$ spectral irradiance in energy units ($W\,m^{-2}\,nm^{-1}$)

$I^{Q}(\lambda)$ spectral irradiance in quantum units ($\mu mol\,m^{-2}\,s^{-1}\,nm^{-1}$)

I_{E}^{E} integral energy irradiance in energy units ($W\,m^{-2}$)

I_{E}^{Q} integral energy irradiance in quantum units ($\mu mol\,m^{-2}\,s^{-1}$)

I_{PARE}^{E} integral PAR energy irradiance in energy units ($W\,m^{-2}$)

I_{PARE}^{Q} integral PAR energy irradiance in quantum units ($\mu mol\,m^{-2}\,s^{-1}$)

I_{PARQ}^{E} integral PAR quantum irradiance in energy units ($W\,m^{-2}$)

I_{PARQ}^{Q} integral PAR quantum irradiance in quantum units ($\mu mol\,m^{-2}\,s^{-1}$)

I_{Q}^{E} integral quantum irradiance in energy units ($W\,m^{-2}$)

I_{Q}^{Q} integral quantum irradiance in quantum units ($\mu mol\,m^{-2}\,s^{-1}$)

K^{I} ratio of PAR to the integral radiation

n_{E} integral electrical output of the energy sensor (mV)

$n_{E}(\lambda)$ energy sensor's electrical output in measuring $I^{E}(\lambda)$ (mV)

n_{idE} integral electrical output of the ideal energy sensor (mV)

n_{idQ} integral electrical output of the ideal quantum sensor (mV)

n_{Q} integral electrical output of the quantum sensor (mV)

$n_{Q}(\lambda)$ quantum sensor's electrical output in measuring $I^{Q}(\lambda)$ (mV)

PARE integral energy photosynthetically active radiation ($W\,m^{-2}$; $\mu mol\,m^{-2}\,s^{-1}$)

PARQ integral quantum photosynthetically active radiation ($W\,m^{-2}$; $\mu mol\,m^{-2}\,s^{-1}$)

$R(\lambda)$ spectral reflectance

S direct solar radiation (direct integral irradiance) ($W\,m^{-2}$)

$S(\lambda)$ spectral direct solar radiation (direct spectral irradiance) ($W\,m^{-2}\,nm^{-1}$)

$T(\lambda)$ spectral transmittance

U^{I} conversion factor between integral irradiance in energy and quantum units ($W\,s\,\mu mol^{-1}$)

U_{PAR}^{I} conversion factor between PAR integral irradiance in energy and quantum units ($W\,s\,\mu mol^{-1}$)

β_{E}^{I} spectral correction of the energy sensor relative to the ideal energy sensor in measuring radiation I_{E}

β_{PAR}^{I} spectral correction of PAR sensor in measuring radiation I

β_{PYR}^{I} spectral correction for pyranometer calibrated using pyrheliometer in measuring radiation I

γ $\gamma = N_{A}hc = 119.8$ ($W\,s\,nm\,\mu mol^{-1}$)

ε_{E}^{E} integral sensitivity of energy sensor in energy units ($mV\,m^{2}\,W^{-1}$)

$\varepsilon_{E}^{E}(\lambda)$ spectral sensitivity of energy sensor in energy units ($mV\,m^{2}\,nm\,W^{-1}$)

ε_{E}^{Q} integral sensitivity of energy sensor in quantum units ($mV\,m^{2}\,s\,\mu mol^{-1}$)

$\varepsilon_{E}^{Q}(\lambda)$ spectral sensitivity of energy sensor in quantum units ($mV\,m^{2}\,s\,nm\,\mu mol^{-1}$)

$\varepsilon_{idE}^{E}(\lambda)$ spectral sensitivity of ideal energy sensor in energy units ($mV\,m^{2}\,nm\,W^{-1}$)

$\varepsilon_{idE}^{Q}(\lambda)$ spectral sensitivity of ideal energy sensor in quantum units ($mV\,m^{2}\,s\,nm\,\mu mol^{-1}$)

$\varepsilon_{idQ}^{E}(\lambda)$ spectral sensitivity of ideal quantum sensor in energy units ($mV\,m^{2}\,nm\,W^{-1}$)

$\varepsilon_{idQ}^{Q}(\lambda)$ spectral sensitivity of ideal quantum sensor in quantum units ($mV\,m^{2}\,s\,nm\,\mu mol^{-1}$)

ε_{PARE}^{E} integral sensitivity of PAR energy sensor in energy units ($mV\,m^{2}\,W^{-1}$)

ε_{PARE}^{Q} integral sensitivity of PAR energy sensor in quantum units ($mV\,m^{2}\,s\,\mu mol^{-1}$)

ε_{PARQ}^{E} integral sensitivity of PAR quantum sensor in energy units ($mV\,m^{2}\,W^{-1}$)

ε_{PARQ}^{Q} integral sensitivity of PAR quantum sensor in quantum units ($mV\,m^{2}\,s\,\mu mol^{-1}$)

ε_{Q}^{E} integral sensitivity of quantum sensor in energy units ($mV\,m^{2}\,W^{-1}$)

$\varepsilon_{Q}^{E}(\lambda)$ spectral sensitivity of quantum sensor in energy units ($mV\,m^{2}\,nm\,W^{-1}$)

$\varepsilon_{\mathrm{Q}}^{\mathrm{Q}}$ integral sensitivity of quantum sensor in quantum units ($\mathrm{mV\,m^2\,s\,\mu mol^{-1}}$)

$\varepsilon_{\mathrm{Q}}^{\mathrm{Q}}(\lambda)$ spectral sensitivity of quantum sensor in quantum units ($\mathrm{mV\,m^2\,s\,nm\,\mu mol^{-1}}$)

$\bar{\varepsilon}_{\mathrm{E}}^{\mathrm{E}}(\lambda)$ relative spectral sensitivity of energy sensor in respect of ideal energy sensor

$\bar{\varepsilon}_{\mathrm{E}}^{\mathrm{Q}}(\lambda)$ relative spectral sensitivity of energy sensor in respect of ideal quantum sensor

$\bar{\varepsilon}_{\mathrm{PAR}}^{\mathrm{E}}(\lambda)$ relative spectral sensitivity of PAR sensor in respect of ideal energy sensor

$\bar{\varepsilon}_{\mathrm{PAR}}^{\mathrm{Q}}(\lambda)$ relative spectral sensitivity of PAR sensor in respect of ideal quantum sensor

$\bar{\varepsilon}_{\mathrm{PARQ}}^{\mathrm{E}}(\lambda)$ relative spectral sensitivity of PAR quantum sensor in respect of ideal energy sensor

$\bar{\varepsilon}_{\mathrm{PARQ}}^{\mathrm{Q}}(\lambda)$ relative spectral sensitivity of PAR quantum sensor in respect of ideal quantum sensor

$\bar{\varepsilon}_{Q}^{\mathrm{E}}(\lambda)$ relative spectral sensitivity of quantum sensor in respect of ideal energy sensor

$\bar{\varepsilon}_{Q}^{\mathrm{Q}}(\lambda)$ relative spectral sensitivity of quantum sensor in respect of ideal quantum sensor

$\varepsilon_{\mathrm{idQ}}^{\mathrm{E}}(\lambda)$ relative spectral sensitivity of ideal quantum sensor in respect of ideal energy sensor

λ wave length (nm)

μ_{E} spectral sensitivity of the ideal energy sensor ($\mathrm{mV\,m^2\,nm\,W^{-1}}$)

μ_{Q} spectral sensitivity of the ideal quantum sensor ($\mathrm{mV\,m^2\,s\,nm\,\mu mol^{-1}}$)

χ^{I} PAR quantum efficiency for radiation I ($\mathrm{\mu mol\,W^{-1}\,s^{-1}}$)

Acknowledgements

The research was supported by the ESF Grant No. 2661. The authors thank Mr. Matti Mõttus and Mr. Enn-Märt Maasik for assistance and Mrs. Viivi Randmets and Mrs. Ester Jaigma for preparing the manuscript. The spectral sensitivity of PAR sensors and LI-COR LI-200SA Pyranometer Sensor and the spectral irradiance of calibration lamps were kindly provided to us by LI-COR and Kipp and Zonen firms. The regional editor of the journal Dr. J. B. Stewart and the anonymous reviewers are highly acknowledged for their comments and suggestions in improving the manuscript.

References

Alados, I., Foyo-Moreno, I., Alados-Arboledas, L., 1995. Photosynthetically active radiation: measurements and modelling. Agric. For. Meteorol. 78, 121–131.

Avaste, O., Moldau, H., Shifrin, K.S., 1962. Spectral distribution of direct solar and diffuse radiation. In: Investig. Atm. Phys. Inst. Phys. Astron. Acad. Sci. E.S.S.R. Tartu, 3, pp. 23–71 (in Russian).

Bird, R.E., Hulstrom, R.L., Kliman, A.W., Eldering, H.G., 1982. Solar spectral measurements in the terrestrial environment. Appl. Opt. 21, 1430–1436.

Bird, R.E., Hulstrom, R.L., Lewis, J.L., 1983. Terrestrial solar spectra data sets. Solar Energy 30, 563–573.

Bird, R.E., 1984. A simple solar spectral model for direct-normal and diffuse horizontal irradiance. Solar Energy 32, 461–471.

Bird, R.E., Riordan, C., 1986. Simple solar spectral model for direct and diffuse irradiance on horizontal and tilted planes at the Earth's surface for cloudless atmospheres. J. Climate Appl. Meteorol. 25, 87–97.

Bishnoi, P., Sedgley, P.R.H., 1985. Spectral analysis of transmitted radiation in summer crops in a mediterranean climate. Int. J. Ecol. Environ. Sci. 11, 55–67.

Blackburn, W.J., Proctor, J.T.A., 1983. Estimating photosynthetically active radiation from measured solar irradiance. Solar Energy 31, 233–234.

Britton, C.M., Dodd, J.D., 1976. Relationships of photosynthetically active radiation and shortwave irradiance. Agric. Meteorol. 17, 1–7.

Czarnowski, M., 1994a. Spectral composition of solar irradiation incident upon plant ecosystems. Zeszyty Problemove Postepów Nauk Rolniczych 405, 21–31.

Czarnowski, M., 1994b. Spectral properties of tree leaves. Zeszyty Problemove Postepów Nauk Rolniczych 405, 43–54.

Czarnowski, M., Cebula, St., 1996. Effect of leaf area index on spectral transmittance of solar radiation in greenhouse cultivation of sweet pepper plants. Folia Hortic. 8/1, 53–72.

Deering, D.W., Leone, A., 1986. A sphere-scanning radiometer for rapid directional measurements of sky and ground radiance. Remote Sens. Environ. 19, 1–24.

Endler, J.A., 1993. The color of light in forests and its implications. Ecol. Monographs 63, 1–27.

Gaastra, P., 1959. Photosynthesis of crop plants as influenced by light, carbon dioxide, temperature, and stomatal diffusion resistance. Mededelingen van de Landbouwhogeschool te Wageningen, Netherland, 59, pp. 1–68.

Gueymard, C., 1989. An atmospheric transmittance model for the calculation of the clear sky beam, diffuse and global photosynthetically active radiation. Agric. For. Meteorol. 45, 215–229.

Hansen, V., 1984. Spectral distribution on clear days: a comparison between measurements and model estimates. J. Climate Appl. Meteorol. 23, 772–780.

Henderson, S.T., Hodgkiss, D., 1963. Spectral energy distribution of daylight. Brit. J. Appl. Phys. 14, 125–131.

Howell, T.A., Meek, D.W., Hatfield, J.L., 1983. Relationship of photosynthetically active radiation to shortwave in the San Joaquin Valley. Agric. Meteorol. 28, 157–175.

Jacovides, C.P., Kallos, G.B., Steven, M.D., 1993. Spectral band resolution of solar radiation in Athens, Greece. Int. J. Climatol. 13, 689–697.

Jacovides, C.P., Timbios, F., Asimakopoulus, D.N., Steven, M.D., 1997. Urban aerosol and clear skies spectra of global and diffuse photosynthetically active radiation. Agric. For. Meteorol. 87, 91–104.

Jacquemoud, S., Baret, F., 1990. PROSPECT: a model of leaf optical properties spectra. Remote Sens. Environ. 34, 75–91.

Jacquemoud, S., 1993. Inversion of the PROSPECT +SPAIL canopy reflectance model from AVIRIS equivalent spectra: theoretical study. Remote Sens. Environ. 44, 281–292.

Karalis, J.D., 1989. Characteristics of direct photosynthetically active radiation. Agric. For. Meteorol. 48, 225–234.

Kylling, A., 1993. Radiation transport in cloudy and aerosol loaded atmospheres 1. Radiative fluxes at the Earth surface under cloudy conditions. In: Rep. Series in Aerosol Sci. Finnish Assoc. for Aerosol Research No. 21, pp. 28–35.

Lee, D.W., Graham, R., 1986. Leaf optical properties of rainforest sun and extreme shade plants. Am. J. Bot. 73, 1100–1108.

Lee, D.W., 1987. Spectral distribution of radiation in two neotropical forests. Biotropica 19, 161–166.

Lee, D.W., Downum, K.R., 1991. Spectral distribution of biologically active solar radiation at Miami, Florida, USA. Int. J. Biometeorol. 35, 48–54.

Lemeur, R., Rosenberg, N.J., 1979. Simulating the quality and quantity of short-wave radiation within and above canopies. In: Comparison of Forest Water and Energy Exchange Models. Int. Soc. for Ecol. Modelling, Copenhagen, 1979, pp. 77–100.

LI-COR, 1986. LI-COR Radiation Sensors. Instruction manual. Publ. No. 8609-56, Lincoln, Nebraska, USA.

LI-COR, 1991. LI-COR Radiation Measurement Instruments. Lincoln, Nebraska, USA.

Lorenzen, B., Jensen, A., 1991. Spectral properties of a barley canopy in relation to spectral properties of single leaves and the soil. Remote Sens. Environ. 37, 23–34.

McCree, K.J., 1966. A solarimeter for measuring photosynthetically active radiation. Agric. Meteorol. 3, 353–366.

McCree, K.J., 1972a. Test of current definitions on photosynthetically active radiation against leaf photosynthesis data. Agric. Meteorol. 10, 443–453.

McCree, K.J., 1972b. The action spectrum, absorptance and quantum yield of photosynthesis in crop plants. Agric. Meteorol. 9, 191–216.

McCree, K.J., 1973. The measurement of photosynthetically active radiation. Solar Energy 15, 83–87.

McCree, K.J., 1976. A comparison of experimental and theoretical spectra for photosynthetically active radiation at various atmospheric turbidities. Agric. Meteorol. 16, 405–412.

Meek, D.W., Hatfield, J.L., Howell, T.A., Idso, S.B., Reginato, R.J., 1984. A generalized relationship between photosynthetically active radiation and solar radiation. Agron. J. 76, 939–945.

Moldau, H., Ross, J., Tooming, H., Undla, I., 1963. Geographic distributions of photosynthetically active radiation (PAR) over the European territory of the U.S.S.R. In: Photosynthesis and Problems of Plant Productivity. USSR Acad. Sci., Moscow, pp. 149–158 (in Russian).

Nichiporovich, A.A., 1960. Conference on measurement of visible radiation in plant physiology, Soviet Plant Physiol., 7, pp. 744–747 (in Russian).

Niilisk, H., 1962. Simplified spectrophotometer for measurements of spectral fluxes of diffuse radiation. In: Investig. Atm. Phys. Inst. Phys. Astron. Acad. Sci. E.S.S.R., Tartu, 3, pp. 150–159 (in Russian).

Niilisk, H., 1965. Spectrophotometer for measuring spectral radiation fluxes in plant cover. In: Proc. Estonian Acad. Sci., Ser. Phys. Math. Technol., 14, pp. 528–553 (in Russian).

Norman, J.M., Tanner, C.B., Thurtell, G.W., 1969. Photosynthetic light sensor for measurements in plant canopies. Agron. J. 61, 840–843.

Olseth, J.A., Skartveit, A., 1997. Spatial distribution of photosynthetically active radiation over complex topography. Agric. For. Meteorol. 86, 205–214.

PAR LITE, 1999. Sensor for photosynthetic photon flux. SCI-TEC Instruments/Kipp and Zonen. Newsletter.

Papaioannou, G., Nikolidakis, G., Asimakopoulus, D.N., Redalis, D., 1996. Photosynthetically active radiation in Athens. Agric. For. Meteorol. 81, 287–298.

Pearcy, R.W., 1989. Radiation and light measurements. In: Pearcy, R.W., Ehleringer, J.E., Mooney, H.A., Rundel, P.W. (Eds.), Plant Physiological Ecology: Field Methods and Instrumentation. Chapman & Hall, London, pp. 97–116.

Rao, C.R., 1984. Photosynthetically active components of global solar radiation: measurements and model computations. Arch. Met. Geophys. Bioclim., Ser. B. 34, 353–364.

Rodskjer, N., Kornher, A., 1971. Über die Bestimmung der Strahlungsenergie im Wellenlängebereich von 0.3–0.7 μ in Pflanzenbeständen. Agric. Meteorol. 8, 139–150.

Romero, J., Wehrli, C., Frohlich, C., 1996. Maintenance of the world radiometric reference. In: Int. Pyrheliometric Comparison IPC VIII 25 September–13 October 1995, Results Symp. Swiss Meteorol. Inst. Davos and Zürich, Working Rep. No. 188, pp. 49–51.

Ross, J., 1957. About radiation measurement with Yanishevsky pyranometers. Proc. Acad. Sci. Estonian SSR. Ser. Technol. Phys. Math. Sci. 6, 3–18.

Ross, J., 1981. Radiation Regime and Architecture of Plant Stands. Dr. W. Junk Publishers, The Hague-Boston, London.

Ross, M.S., Flanagan, L.B., La Roi, B.H., 1986. Seasonal and successional changes in light quality and quantity in the understorey of boreal forest ecosystems. Can. J. Bot. 64, 2792–2799.

Ross, J., Ross, V., 1998. Statistical description of the architecture of a fast growing willow coppice. Agric. For. Meteorol. 91, 23–37.

Ross, J., Sulev, M., Saarelaid, P., 1998. Statistical treatment of PAR variability and its application to willow coppice. Agric. For. Meteorol. 91, 1–21.

Satterwhite, M.B., Henley, J.P., 1990. Hyperspectral signatures (400–2500 nm) of vegetation, minerals, soils, rocks, and culture

features: laboratory and field measurements. U.S. Army Crops Engineers. Engineer Topographic Laboratories Fort Belvoir, Virginia, 22060–5546.

Scott, D., Menalda, P.H., Brougham, R.W., 1968. Spectral analysis of radiation transmitted and reflected by different vegetations NZ. J. Bot. 6, 424–449.

Shibayama, M., Akiyama, T., 1989. Seasonal visible, near-infrared and mid-infrared spectra of rice canopies in relation to LAI and above-ground dry phytomass. Remote Sens. Environ. 27, 119–127.

Skidmore, A.K., Schmidt, K.S., 1998. Mapping rangeland vegetation using hyperspectral vegetation spectra. In: 1st EARSeL Workshop on Imaging Spectroscopy. EARSEL, Paris, pp. 285–297.

Slomka, J., Slomka, K., 1986. Participation of photosynthetically active radiation in global radiation. Publ. Inst. Geophys. Polish Acad. Sci. D25, 197.

Spitters, C.J.T., Tousaint, H.A.J.M., Goudriaan, J., 1986. Separating the diffuse and direct component of global radiation and its implications for modelling canopy photosynthesis Part 1. Components of incoming radiation. Agric. For. Meteorol. 38, 217–229.

Stanhill, G., Fuchs, M., 1977. The relative flux density of photosynthetically active radiation. J. Appl. Ecol. 14, 317–322.

Stigter, C.J., Musabilha, V.M.M., 1982. The conservation ratio of photosynthetically active to total radiation in the tropics. J. Appl. Ecol. 19, 853–858.

Sulev, M., Ross, J., 1996. Conversion factor between global solar radiation and photosynthetic active radiation. In: Perttu, K., Koppel, A. (Eds.), Short Rotation Willow Coppice for Renewable Energy and Improved Environment. In: Proc. Joint Swedish–Estonian Seminar on Energy Forestry and Vegetation Filters, Tartu, 24–26 September 1995. Swedish Univ. Agric. Sci. Uppsala, Report 57, pp. 115–121.

Tooming, H., 1967. An approximate method for determining the attenuation and reflectation of PAR and near infrared radiation in a maize stand from the measurements of total radiation. In: Nichiporovich, A.A (Ed.), Photosynthesis of Productive Systems. Isr. Progr. for Sci. Transl. Jerusalem, pp. 100–113.

Tooming, H.G., Gulyayev, B.I., 1967. Methods of measurement of photosynthetically active radiation. Nauka, Moscow (in Russian).

Tooming, H., Niilisk, H., 1967. Transition coefficients from integrated radiation to photosynthetic active radiation (PAR) under field conditions. Phytoactinometrical Investigations of Plant Canopy. Valgus, Tallinn, pp. 140–149 (in Russian).

Turner, B., Dibley, G., Dury, S., 1998. Hyperspectral characteristics of Australian native eucalypt forests. In: 1st EARSeL Workshop on Imaging Spectroscopy. EARSEL, Paris, pp. 317–328.

Weiss, A., Norman, J.M., 1985. Partitioning solar radiation into direct and diffuse. Agric. For. Meteorol. 34, 205–213.

Yefimova, N.A., 1965. Distribution of photosynthetically active radiation on the territory of the Soviet Union. Transact. Main Geophys. Obs., Fasc. 179, pp. 118–130 (in Russian).